R&D trends in halide-based single crystal materials

Martin Nikl

Institute of Physics,
Academy of Sciences of the Czech Republic

(nikl@fzu.cz)

Summer school, Universita Milano-Bicocca, September 12-13, 2016

W.C. Roentgen, Science 3, 227 (1896)

*ON A NEW KIND OF RAYS.**

1. A DISCHARGE from a large induction coil is passed through a Hittorf's vacuum tube, or through a well-exhausted Crookes' or Lenard's tube. The tube is surrounded by a fairly close-fitting shield of black paper; it is then possible to see, in a completely darkened room, that paper covered on one side with barium platinocyanide lights up with brilliant fluorescence when brought into the neighborhood of the tube, whether the painted side or the other be turned towards the tube. The fluorescence is still visible at two metres distance. It is easy to show that the origin of the fluorescence lies within the vacuum tube.

Film
30 min.
exp.

Film+$CaWO_4$
30 s exp.

History of scintillators starts short after the discovery of X-rays at the end of 19th century

…

$CaWO_4$ powder in 1896

Bulk single crystals

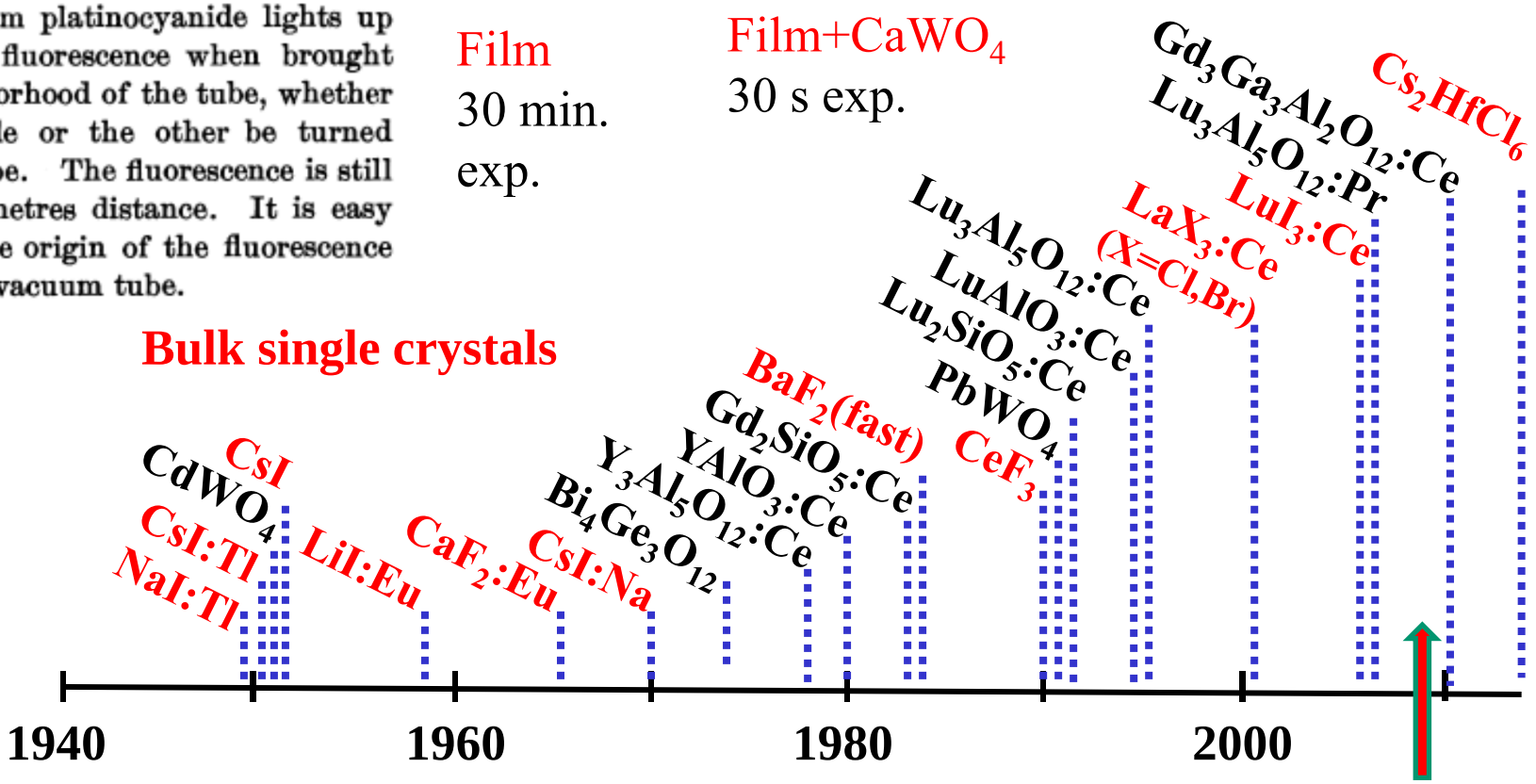

Year of introduction of a scintillation material

Rediscovery of SrI_2:Eu

NaI:Tl, CsI:Tl – the first single crystal scintillators

Introduced at the end of 1940's

Alkali Halide Scintillation Counters

ROBERT HOFSTADTER

Princeton University, Princeton, New Jersey

May 20, 1948

Scintillation flashes of about 1 μs

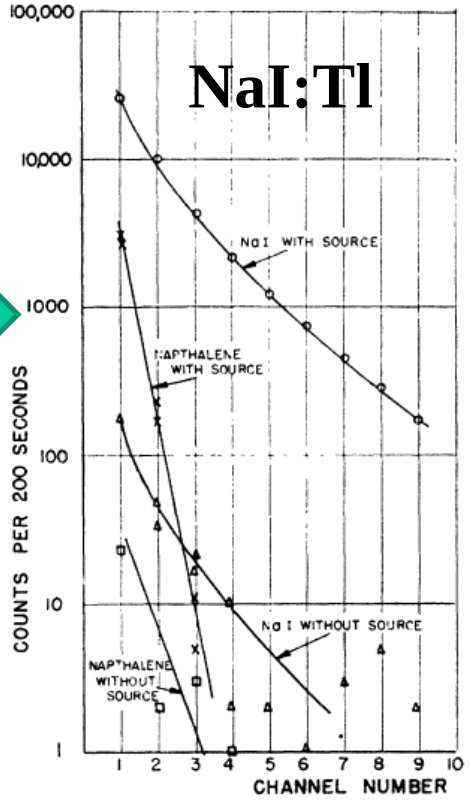

- medium density and good Z_{eff} (ρ=3.67, 4.51 g·cm^{-3}, Z_{eff} = 50.8, 54)

☺

cheap materials, Czochralski or Bridgman growth technique easily applicable

High light yield 40 000 – 60 000 phot/MeV

☹

relatively slow response (300 ns, 1000 ns), worse energy resolution, NaI:Tl hygroscopic

Yet today, widely used in many industrial applications (Nuvia a.s. in Kralupy n/Vlt. produces NaI:Tl)

Single crystals of NaI:Tl

Grown by a Bridgman method in ceramic crucibles, crystals up to 4 inch are readily available

Nuvia a.s., Kralupy n/Vlt.

NaI(Tl) scintilační krystaly, modely SKG a SKW

Thaliem dopované krystaly jodidu sodného jsou nejčastěji používané anorganické scintilátory určené k detekci gama záření. Vedle jejich primárního použití pro detekci a spektrometrii gama záření, se tyto scintilátory také používají pro detekci měkkého rentgenového záření. Díky jejich velkému světelnému výtěžku, vysoké detekční účinnosti a dobrému energetickému rozlišení jsou tyto scintilátory hojně používány v biologii, lékařských aplikacích, geologii, v radionuklidových průmyslových aplikacích, monitorování životního prostředí atd.

Samotné krystaly jodidu sodného jsou vyráběny ze surové taveniny použitím pečlivé a přesně kontrolované techniky růstu. Vypěstované ingoty jsou následně opracovány do standardních rozměrů. Protože je jodid sodný silně hygroskopický, musí být krystaly hermeticky uzavřeny - zapouzdřeny. Luminiscenční světelný výstup je zajištěn předním skleněným okénkem, které je opticky spojeno s krystalem. Zbývající části krystalu jsou pokryty reflexní vrstvou.

Luminescence of NaI:Tl crystals

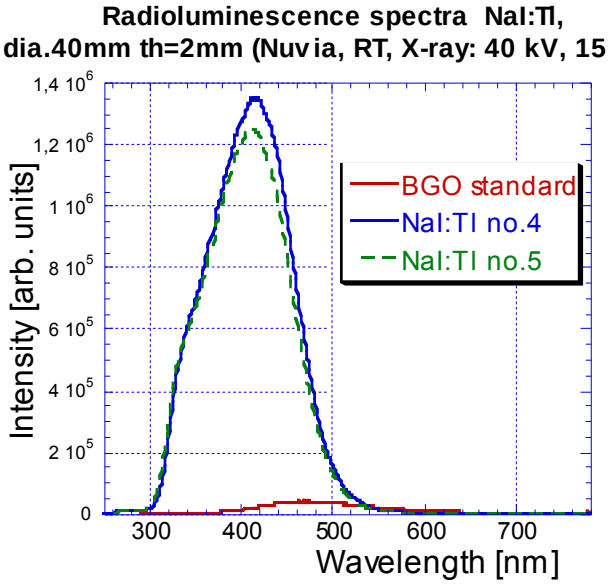

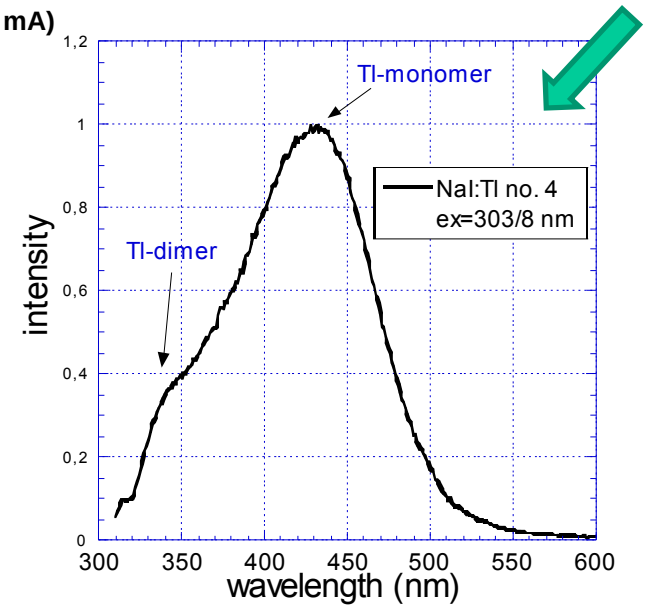

PL emission spectra asymetric at short-wavelength side below 360 nm - Tl-dimer centers at cca 325 nm, monomer Tl+ emits at 420 nm

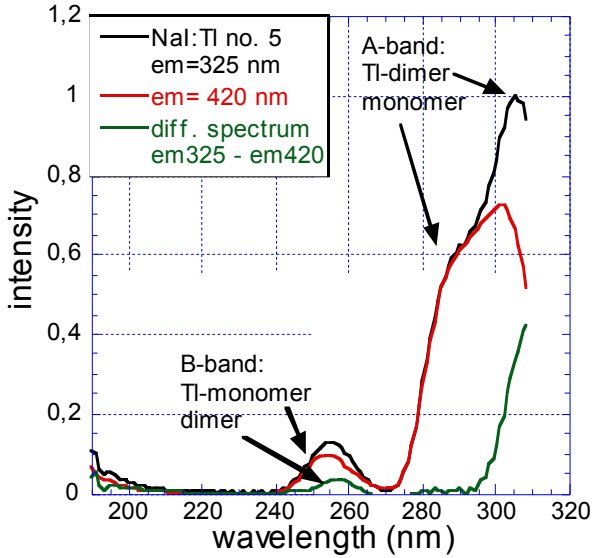

PLE spectra – absorption band of the Tl-monomer center at cca 290-300 nm (A-band, transition 1S0-3P1) and 250-255 nm (B-band, transition 1S0-3P2), whereas for the dimer centers (diff. spectrum in figure) they are at 310 nm and 258 nm, respectively.

Luminescence of CsI:Tl

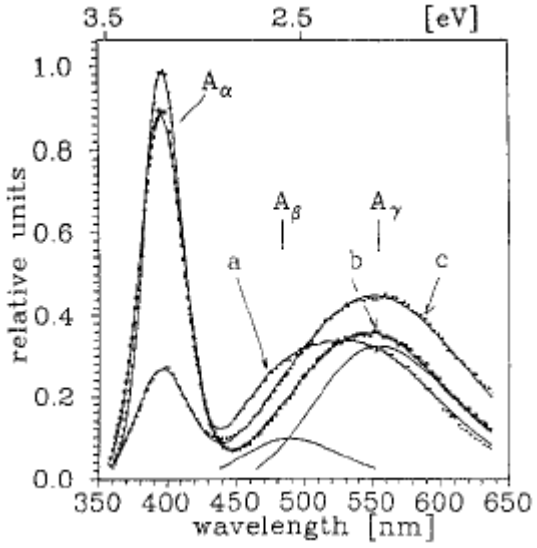

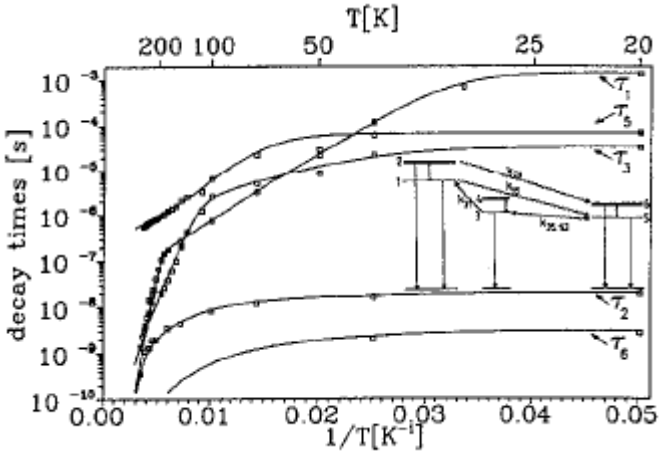

Coexistence of three excited state minima of Tl+ center
Nikl et al, Phil. Mag. ***B67****, 627 (1993)*

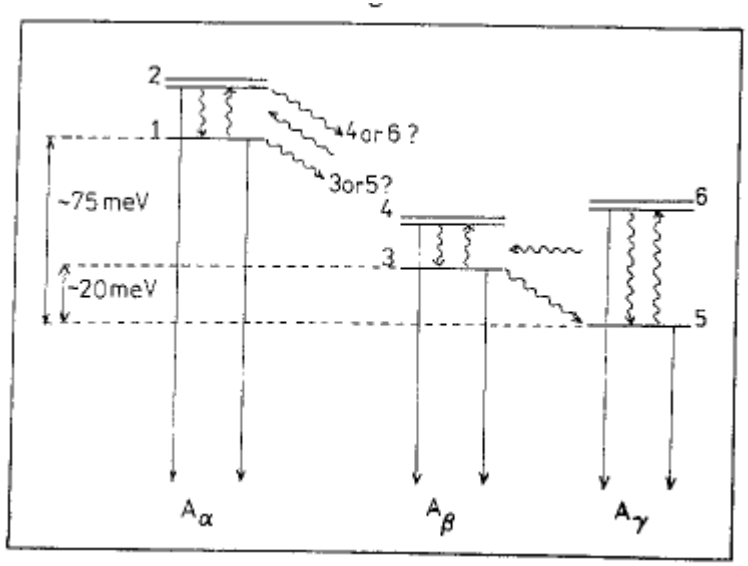

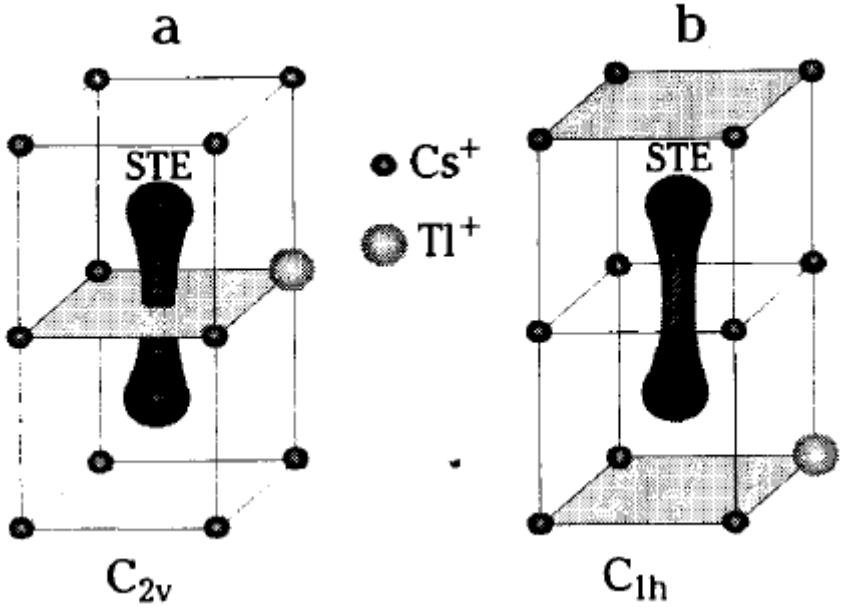

Coexistence of two pairs of Tl^+-like and perturbed exciton minima at APES - new model of luminescence of CsI:Tl (*Nagirnyi et al, CPL* ***227****, 533 (1994)*

Exhibit E-3 Worldwide Radiation Detector Revenues by Application ($ Millions)								
	2011	2012	2013	2014	2015	2016	2017	2
Domestic Security:								
Scintillation	182	190	198	210	223	236	256	
Semiconducting	147	161	177	194	210	232	254	
Thin-film	190	191	192	194	209	225	242	
TOTAL	519	542	567	598	642	693	752	
Military:								
Scintillation	145	151	157	167	177	187	202	
Semiconducting	86	96	106	118	130	145	161	
Thin-film	39	38	38	38	41	44	47	
TOTAL	270	285	301	323	348	376	410	
Medical Imaging:								
Scintillation	239	252	266	284	303	323	349	
Semiconducting	89	97	106	115	122	133	144	
Thin-film	432	415	398	382	413	446	481	
TOTAL	760	764	770	781	838	902	974	1
Nuclear Power:								
Scintillation	81	85	89	94	100	106	115	
Semiconducting	116	128	141	155	167	185	203	
Thin-film	8	8	9	9	10	11	11	
TOTAL	205	221	239	258	277	302	329	
Geophysical:								
Scintillation	83	88	92	98	104	111	120	
Semiconducting	13	15	17	19	21	24	27	
Thin-film	0	0	0	0	0	0	0	
TOTAL	96	103	109	117	125	135	147	
Non-nuclear power scientific and other:								
Geophysical:	109	114	119	126	134	142	154	
Scintillation	138	151	165	181	196	215	236	
Semiconducting	8	8	9	9	10	11	11	
TOTAL	255	273	293	316	340	368	401	
Grand Total	2104	2188	2279	2394	2570	2776	3014	3

Radiation in Medicine **Diagnostics** Basics

Conventional X-Ray Diagnosis
by
Screen / Film Combination

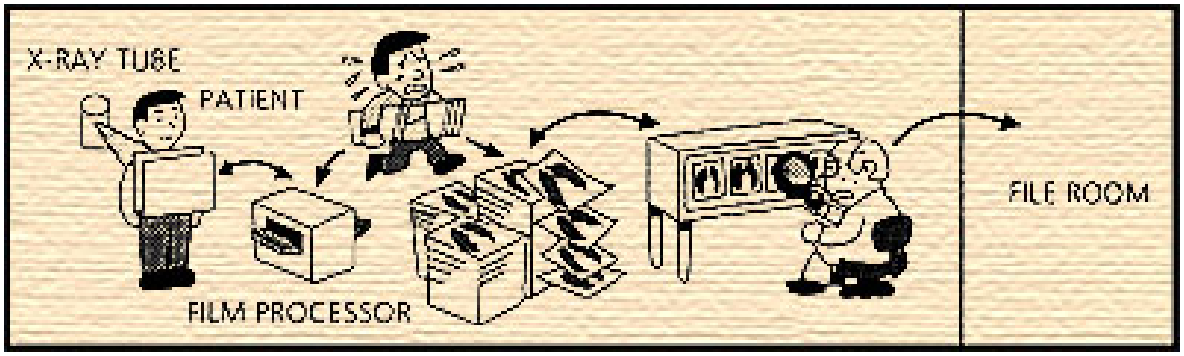

Future X-Ray Diagnosis
by
Computed Radiography System

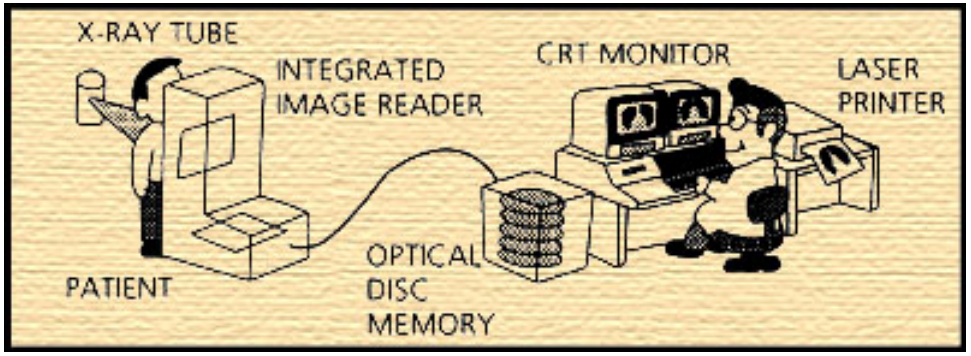

From: Fuji Medical Systems

Digital radiography

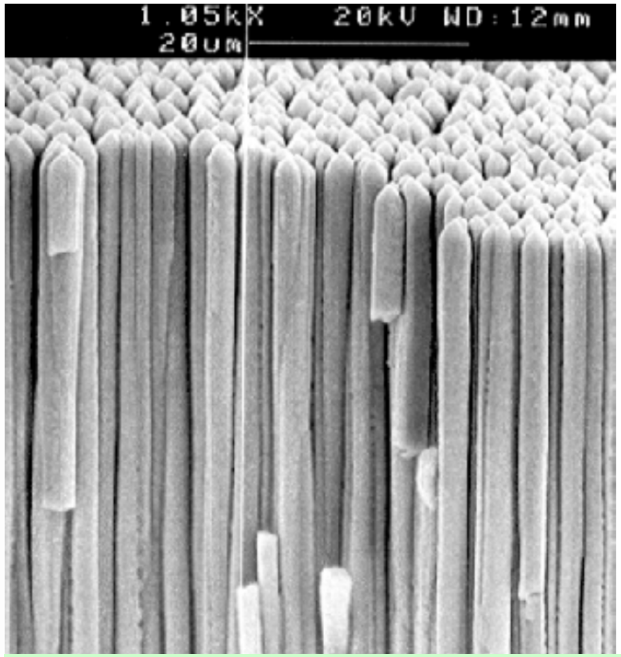

Vapour deposited column-shaped CsI:Tl.
Diameter ~ 3 μm,
length > 0.5 mm.

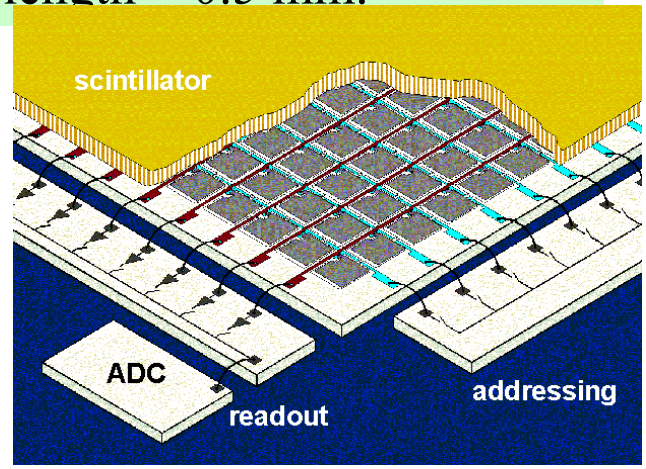

Afterglow suppression in CsI:Tl

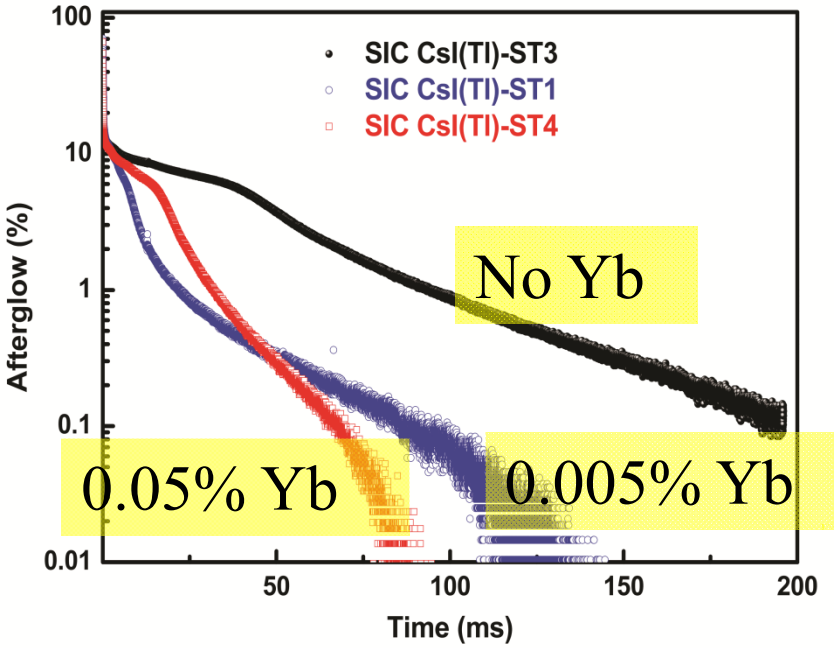

Afterglow profiles of CsI:Tl^{+},Yb^{2+} crystals after X-ray pulse excitation (higher Tl concentration helps further – red curve)

Various codoping strategies were studied (Eu2+, Sm2+, Bi3+) to diminish the afteglow, but LY has been suppresssed as well …..

*Wu et al, CrystEngComm **16**, 3312 (2014)*

Positive role of Yb^{2+} codoping in the afterglow suppression in CsI:Tl crystals was found. In the optimized composition, the CsI:Tl^{+},Yb^{2+} crystal has so far exhibited an ultra-high light yield value of 90,000±6000 photons/MeV, energy resolution 7.9% at 511 keV and suppressed afterglow level down to 0.035% at 80 ms.

Bright halide scintillators in security applications

Around 2000 – LaX3:Ce (X = Cl,Br), in 2008 rediscovered SrI2:Eu2+, now CeBr3 *(low intrinsic radioactivity)*

- Ternary bromine and iodine compounds are searched! (CsBa2I5:Eu, KCaI3:Eu), In+ doping?
- Anion-mixed elpasolites - Cs2NaYBr3I3 and Cs2NaLaBr3I3

Radiation portal monitor

Group of P. Dorenbos and C. L. Melcher have been most active in this field

Crystal	Density [g cm^{-3}]	Bandgap [eV]	Ce^{3+} (Eu^{2+}) 5d–4f emission [nm]	Ce^{3+} (Eu^{2+}) 4f–5d absorption [nm]	Ce (Eu) conc. [mol%]	Scintillation decay time [ns]	LY [10^3 Ph MeV^{-1}]	Energy res. [%] @662 keV
$LaCl_3$:Ce	3.86	7	337,358	243,250,263,274,281	10	24 (60%)	50	3.1
$LaBr_3$:Ce	5.03	5.6	355,390	260,270,284,299,308	5	16	70	2.6
LuI_3:Ce	5.6	n.r.	475,520	≈300,390,419	0.5 2	<50 (50%)	42 (0.5 μs) 51 (10 μs) 58 (0.5 μs) 71 (10 μs)	4.7
$CeBr_3$	5.18	n.r.	370,390	n.r.	100	17	60	4.1
$CeBr_3$:Sr	5.18	n.r.	370,390	n.r.	99.5	17	55	3
$LaBr_3$:Ce,Sr	5.03	5.6	355,390	260,270,284, 299,308	5	18 (78%) 82–2500 (22%)	77	2.0
SrI_2:Eu	4.6	5.5	435	n.r.	5	600–1600	80–120	2.6–3.7
$CsBa_2I_5$:Eu	4.8	n.r.	435	n.r.	7	48 (1%) 383 (6%) 1500 (68%) 9900 (25%)	80–97	3.8

Past, present and future research

Cs_2LiYCl_6:Ce	2003
LuI_3:Ce	2003
K_2LaI_5:Ce	2002
$LaBr_3$:Ce	2001
$LaCl_3$:Ce	2000
$Lu_2Si_2O_7$:Ce	2000
$RbGd_2Br_7$:Ce	1997

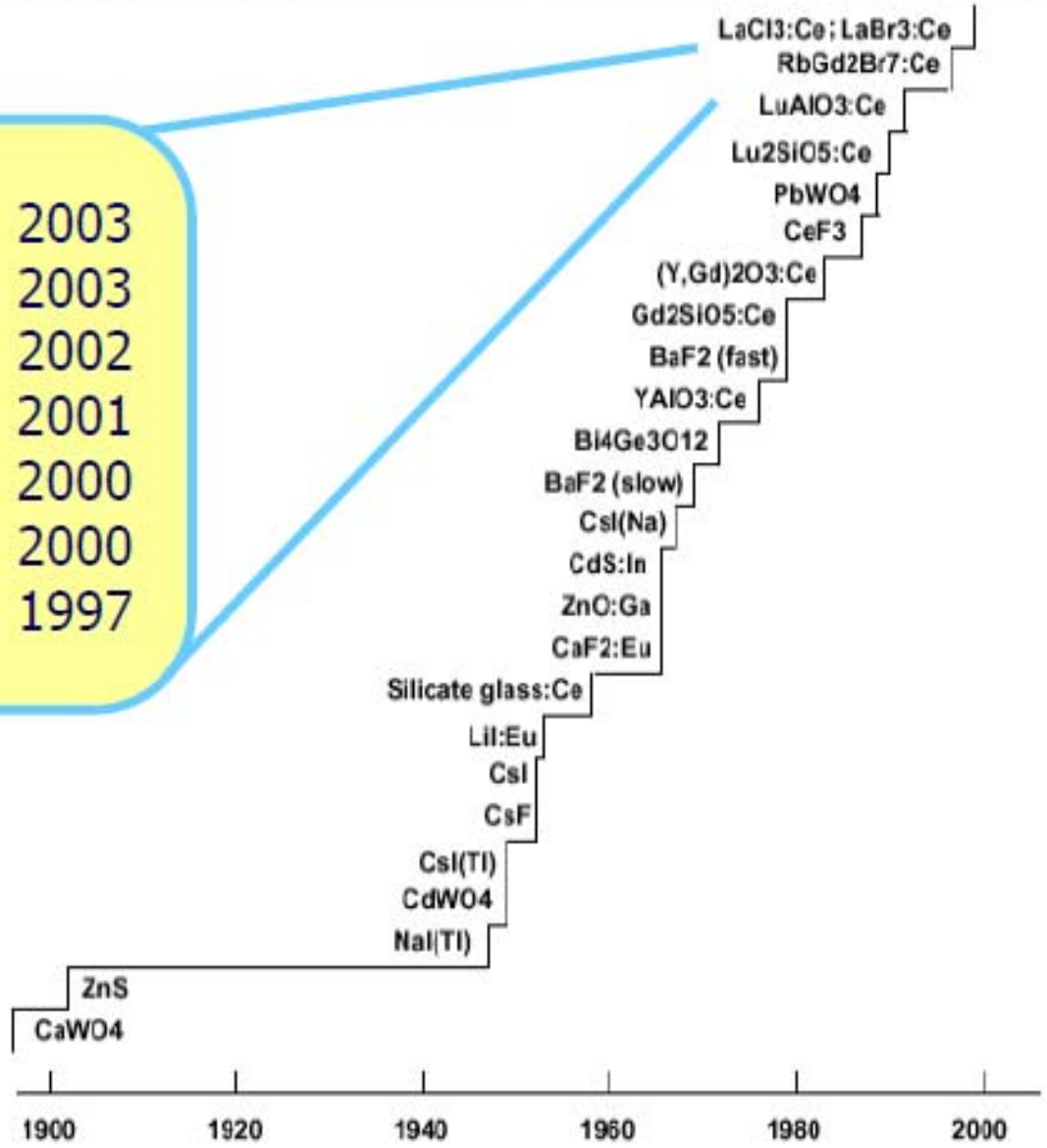

From presentation of P. Dorenbos, KEK, Japan, Nov 11, 2003

Ce-doped LaX_3 (X=Cl,Br) single crystals

LaBr3:Ce: *Van Loef et al, APL 79,1573 (2001)*

LaCl3:Ce: *van Loef et al, IEEE TNS 48, 341 (2001)*

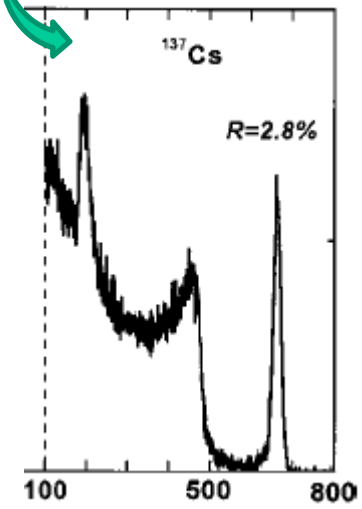

Figure of merit of LaBr3:Ce higher
LY:60-70 000phot/MeV
En.res. 2.8%@667keV

Very hygroscopic!!

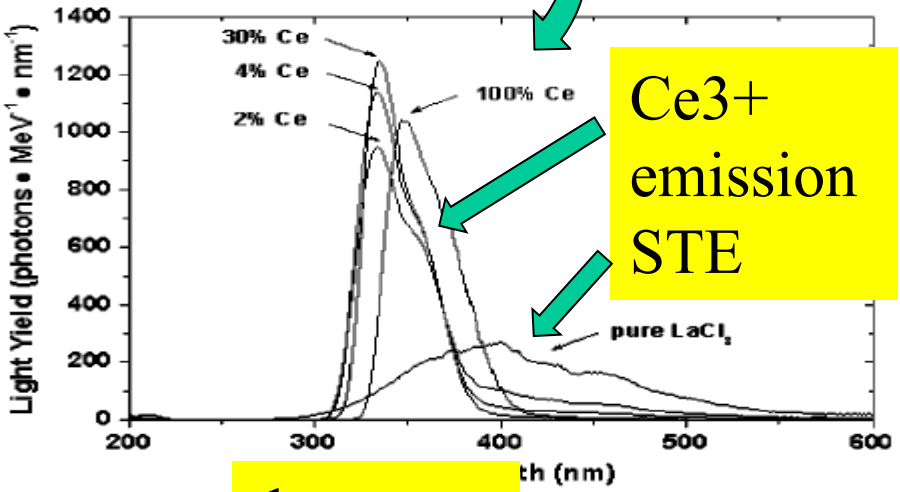

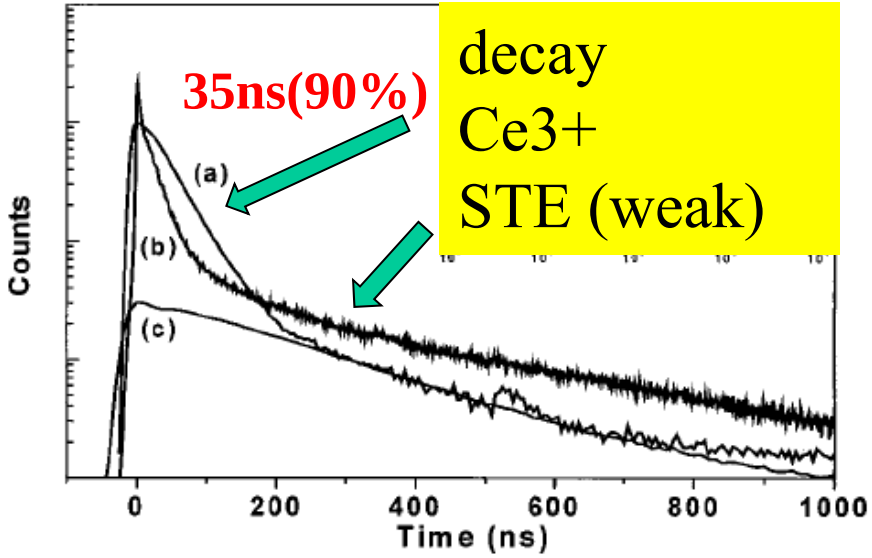

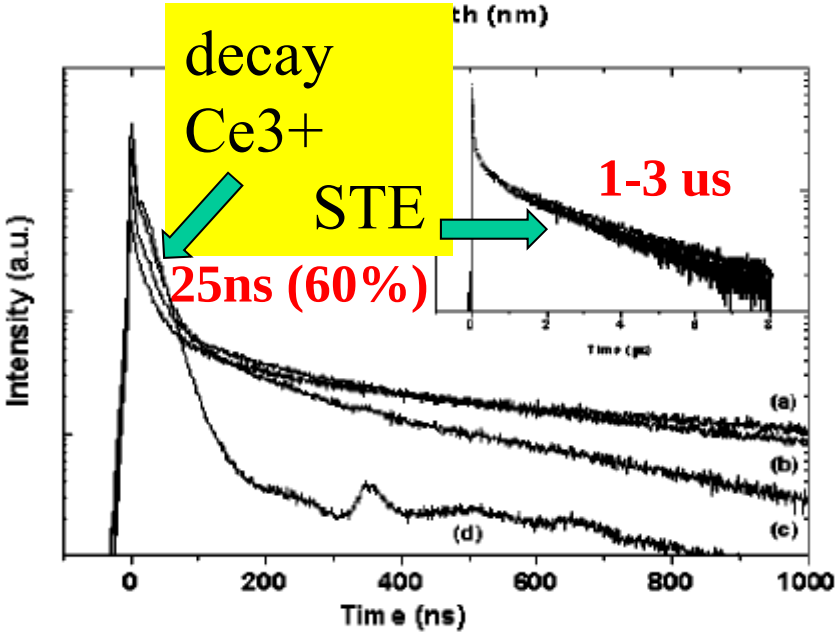

Undoped $LaCl_3$ excitonic emission

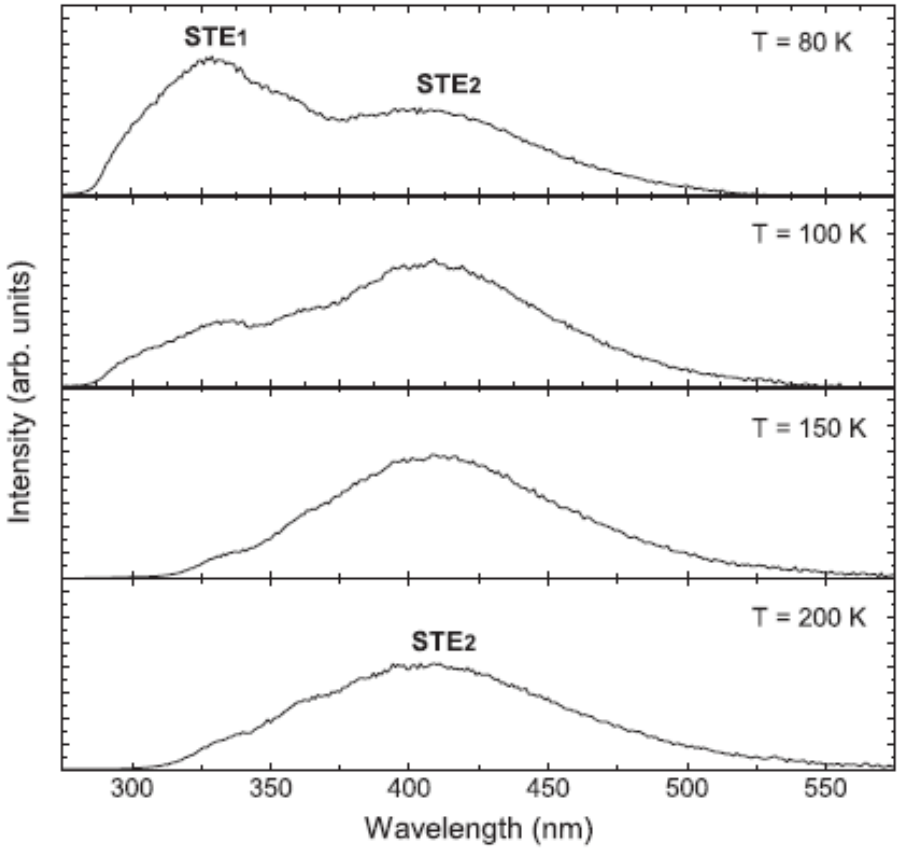

Two emission bands in the X-ray excited emission spectra

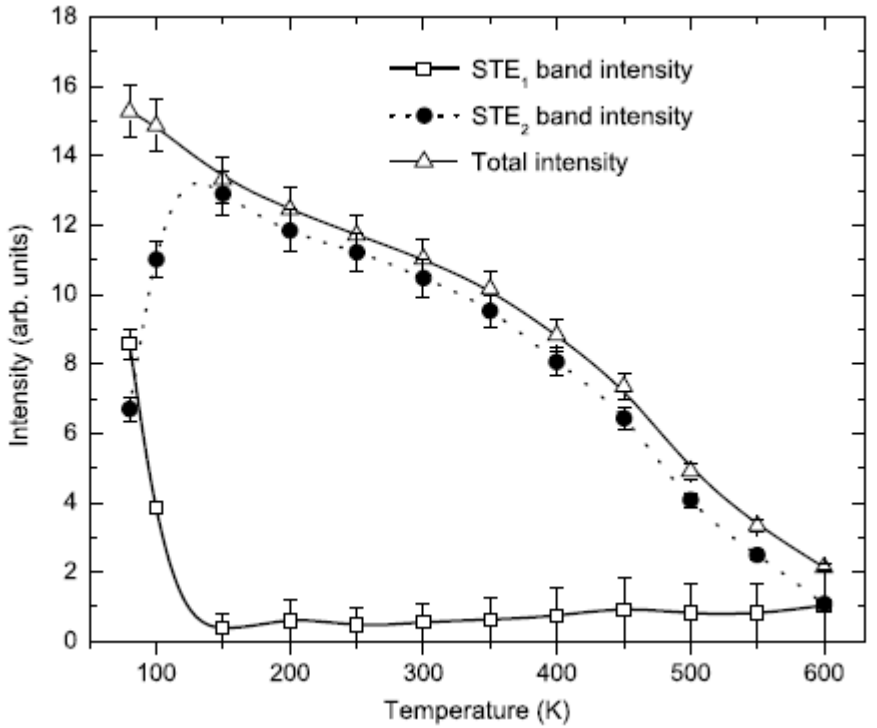

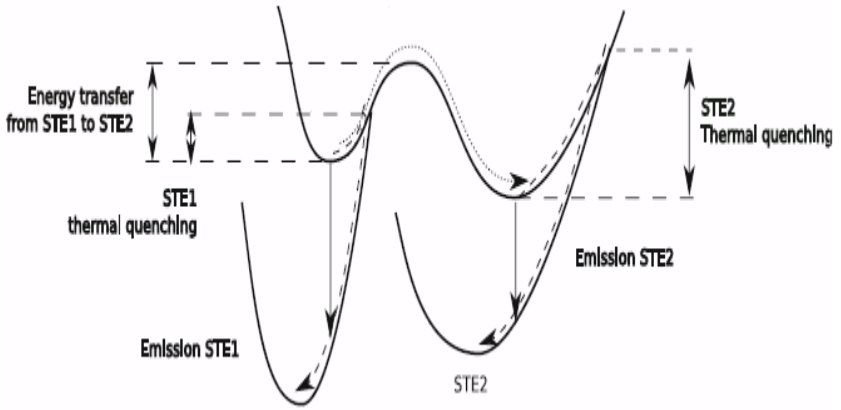

Is really the STE state involved in the energy transfer towards Ce^{3+} centers in scint. Mechanism???

Optimization of $LaBr_3$:Ce by codoping

LaBr3:Ce5%,Sr^{2+}0.03%: *Alekhin et al, APL 102, 161915 (2013)*
LaBr3:Ce, $A^{+}(Me^{2+})$: *Alekhin et al, JAP113, 224904 (2013)*

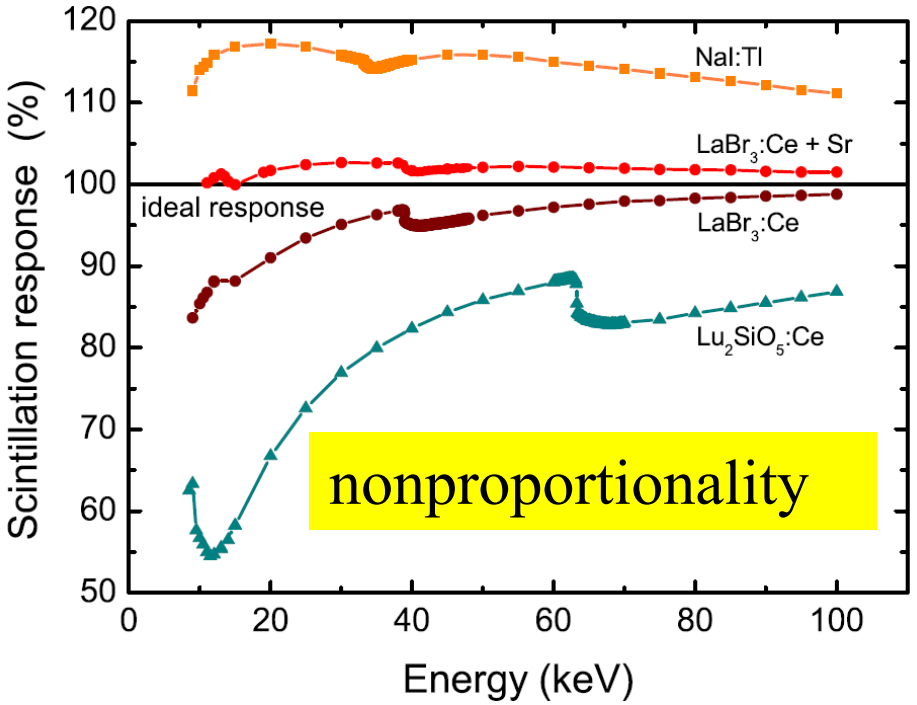

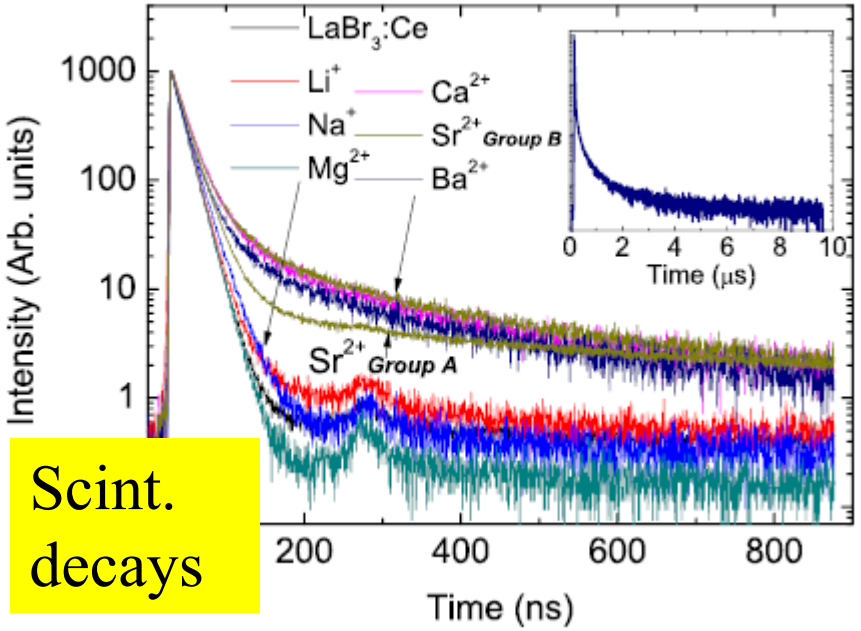

Improved LY up to 78 000 phot/MeV and en.res. up to 2.0%@667keV
Energy resolution improvement explained by smaller nonproportionality, but decay shows slower components, TSL intensity increased, etc., i.e. codoping introduces traps, optimization principle is not clear

5: LaI_3:Ce (recent research)

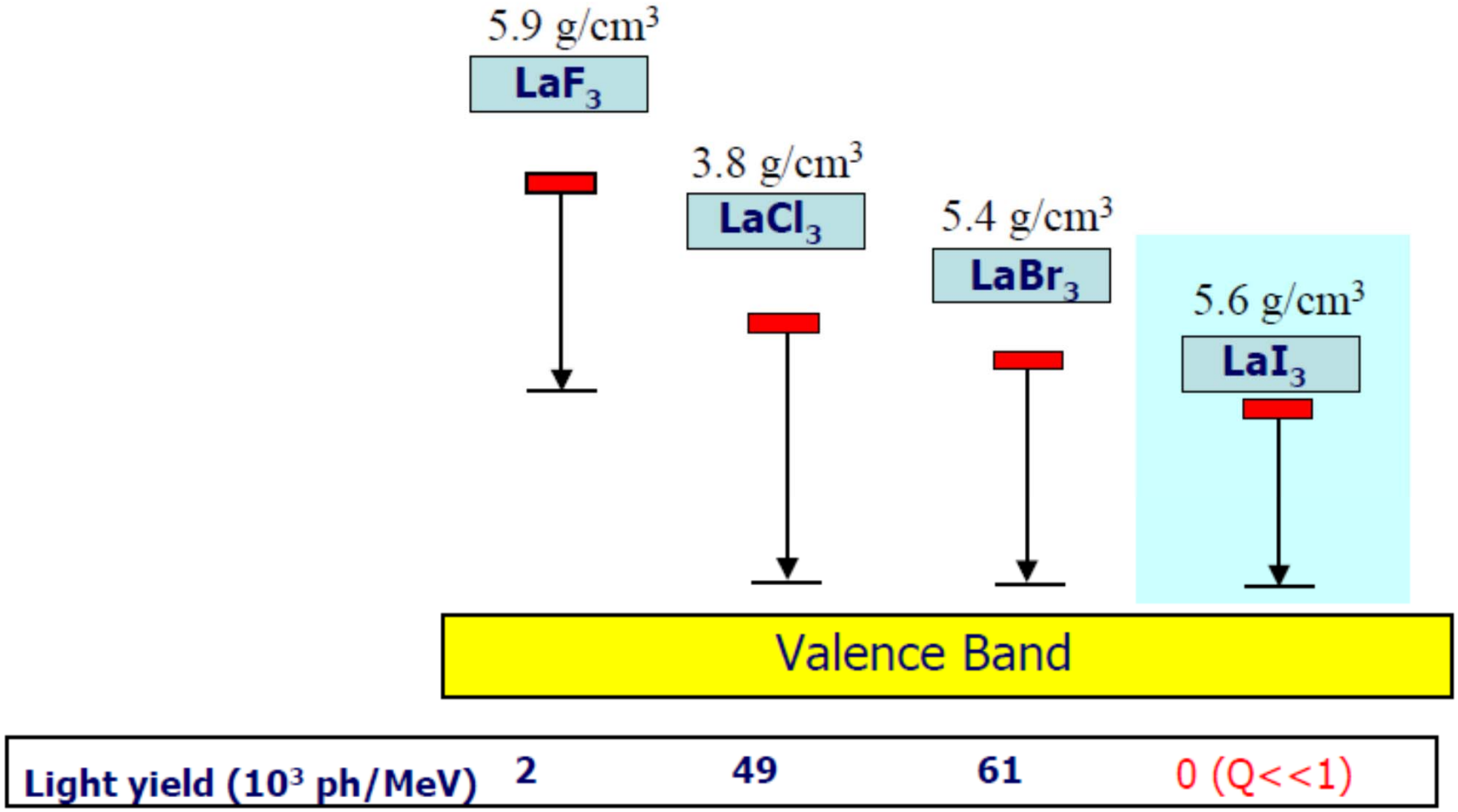

From presentation of P. Dorenbos, KEK, Japan, Nov 11, 2003

Luminescence quenching (Q < 1)

$$\Gamma = \frac{1}{\tau} = \Gamma_v + \Gamma_q$$

$$\Gamma_q(T) = \Gamma_0 \exp\left(\frac{-\Delta E_q}{k_B T}\right)$$

$$I = \frac{\Gamma_v}{\Gamma_v + \Gamma_q}$$

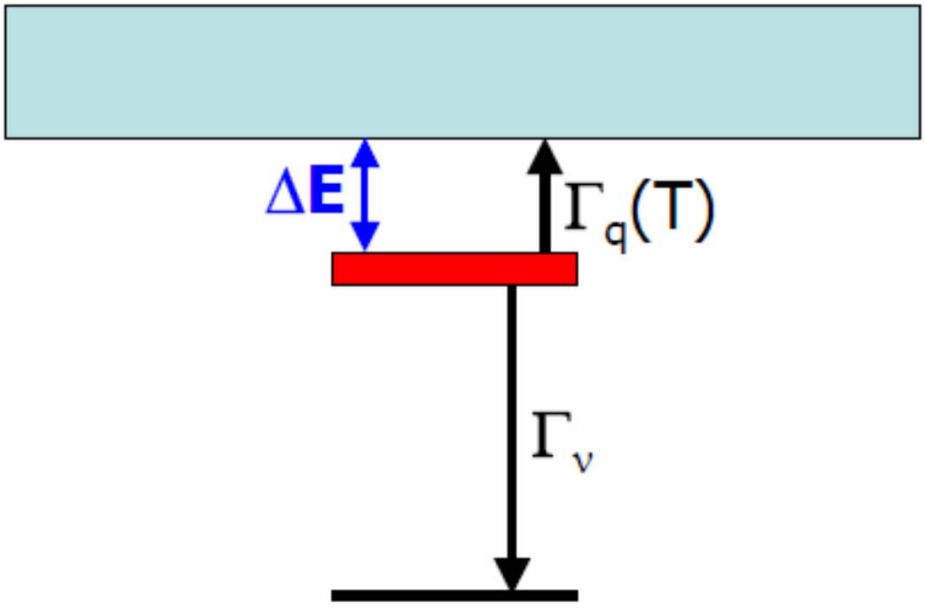

From presentation of P. Dorenbos, KEK, Japan, Nov 11, 2003

LaI_3:Ce; quenching via the conduction band?

Temperature dependence

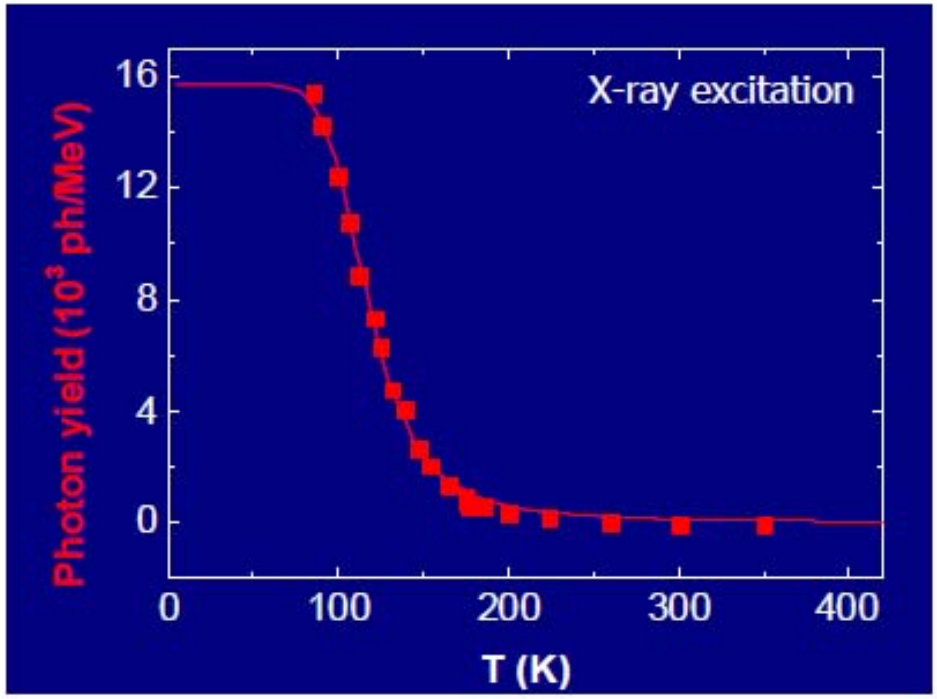

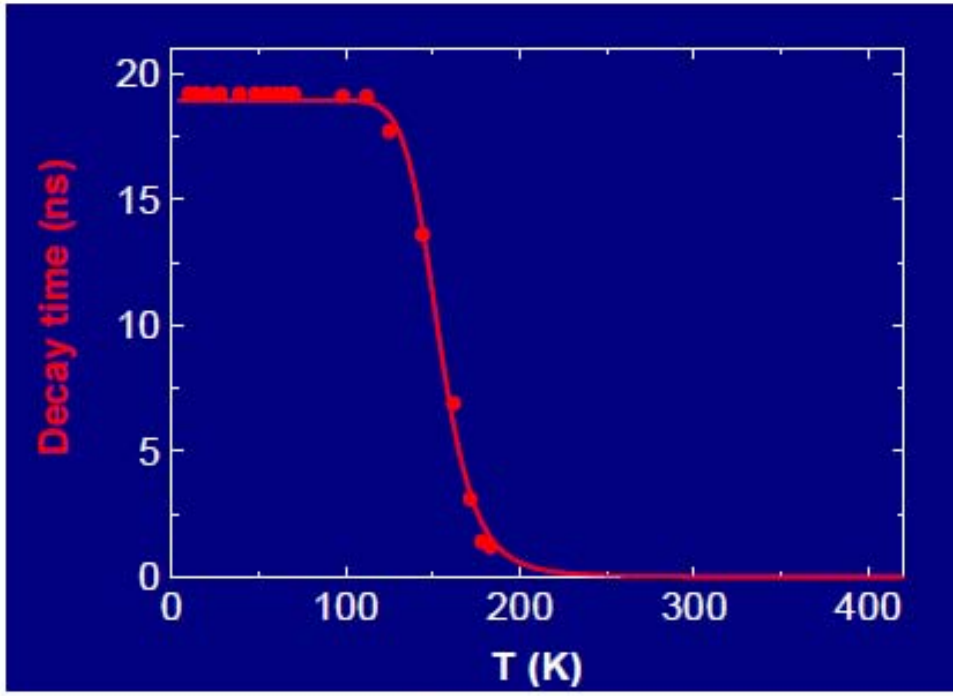

$$I(T)=\frac{I_0}{1+\frac{\Gamma_0}{\Gamma_\nu}\exp\left(-\frac{\Delta E_q}{kT}\right)}$$

➡ ΔE_q=0.08 eV

$$\tau=\frac{1/\Gamma_\nu}{1+\frac{\Gamma_0}{\Gamma_\nu}\exp\left(-\frac{\Delta E_q}{kT}\right)}$$

➡ ΔE_q=0.20 eV

From presentation of P. Dorenbos, KEK, Japan, Nov 11, 2003

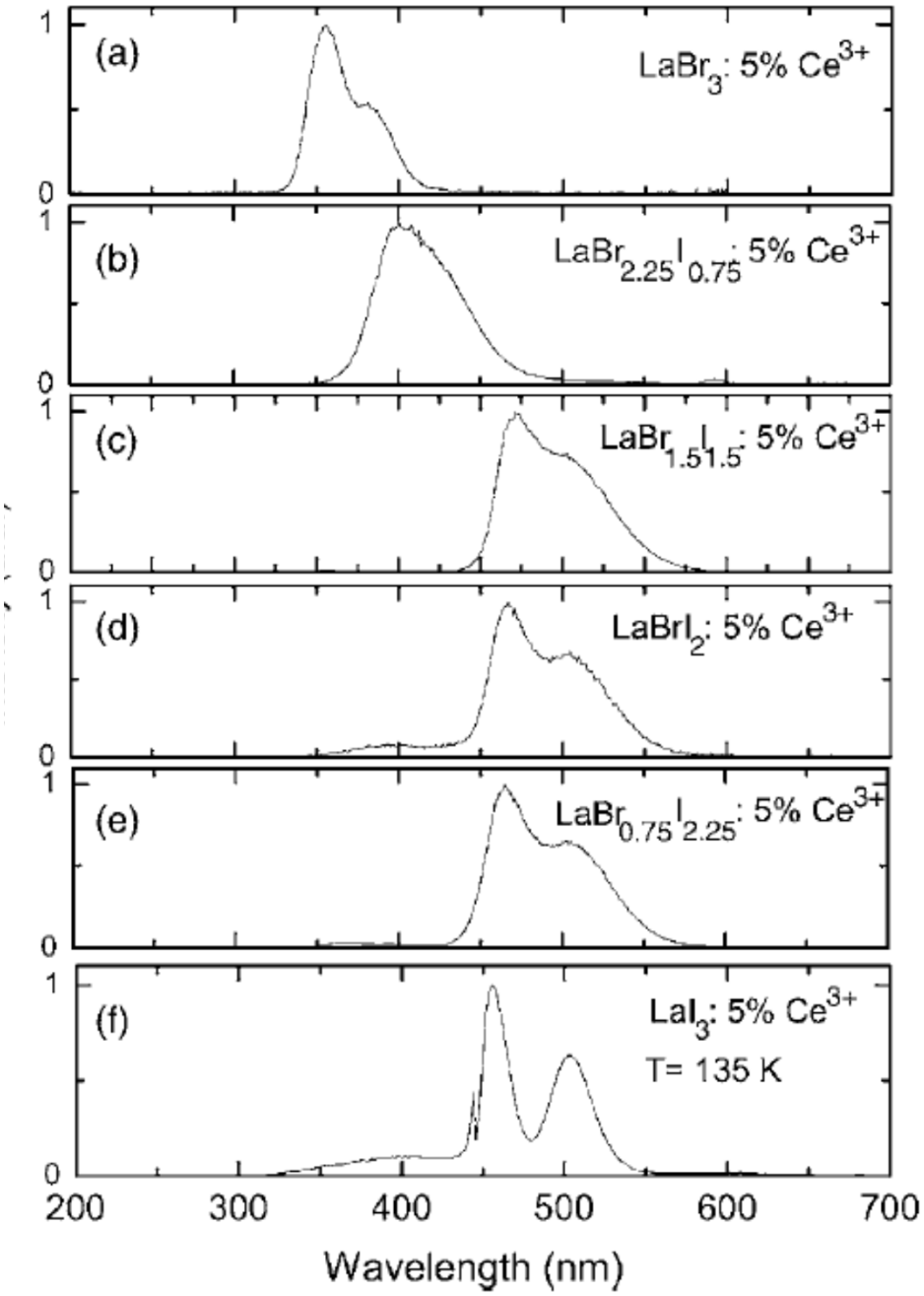

Anion mixed $LaBr_{3-x}I_x$:5%Ce^{3+}

- Inhomogeneous changes in spectra shape and position with anion mixture
- Highest LY value of 58 000 phot/MeV found for x = 1.5
- For x > 1.5 increasing quenching due to ionization of 5d1 state of Ce3+

Birowosuto et al, J. Appl. Physics **103**, 103517 (2008)

6: $LuI_3:Ce^{3+}K_2LaX_5:Ce^{3+}$ (present research)

motivation to study LuI_3:Ce

- Quenching of Ce^{3+} emission via conduction band in LaI_3
- Bandgap of Lu-compounds usually 0.5-1.0 eV larger than La-compounds
- df emission of Ce^{3+} in Lu-compound usually at longer λ than in La-compound

⇒ 5d further below the bottom of the conduction band and larger ΔE_q

From presentation of P. Dorenbos, KEK, Japan, Nov 11, 2003

Ce^{3+} scintillation emission in LaI_3 and LuI_3

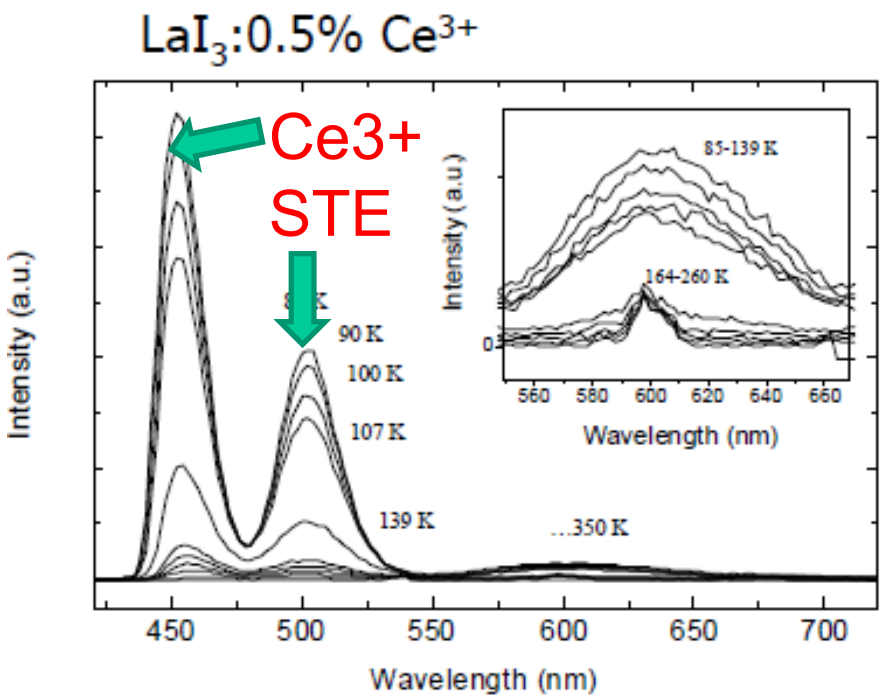

E_g = 3.6 eV

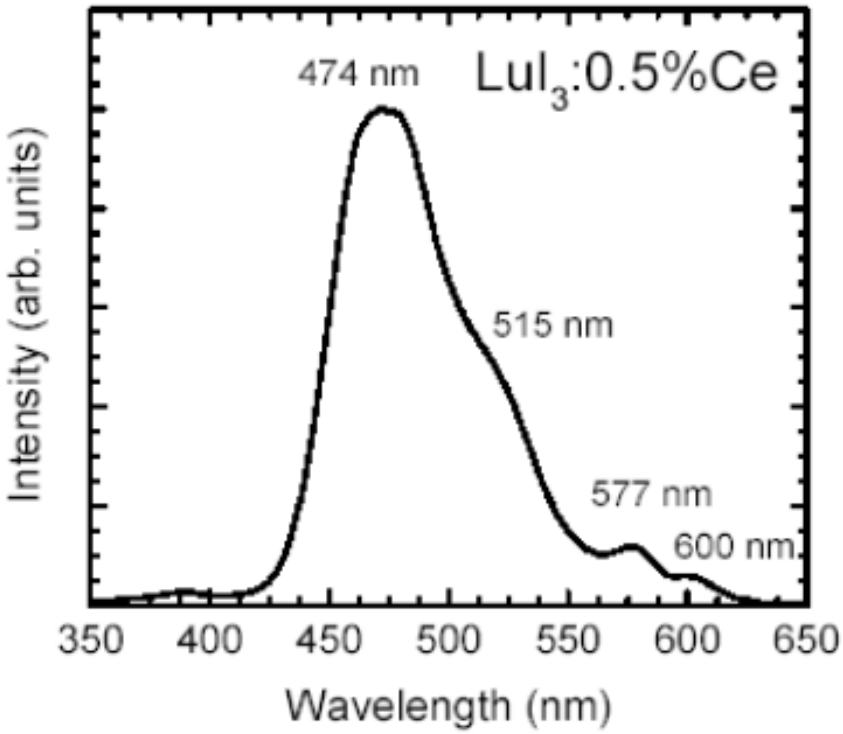

E_g = 4.1 eV

From presentation of P. Dorenbos, KEK, Japan, Nov 11, 2003

Properties of $LuI_3:Ce^{3+}$

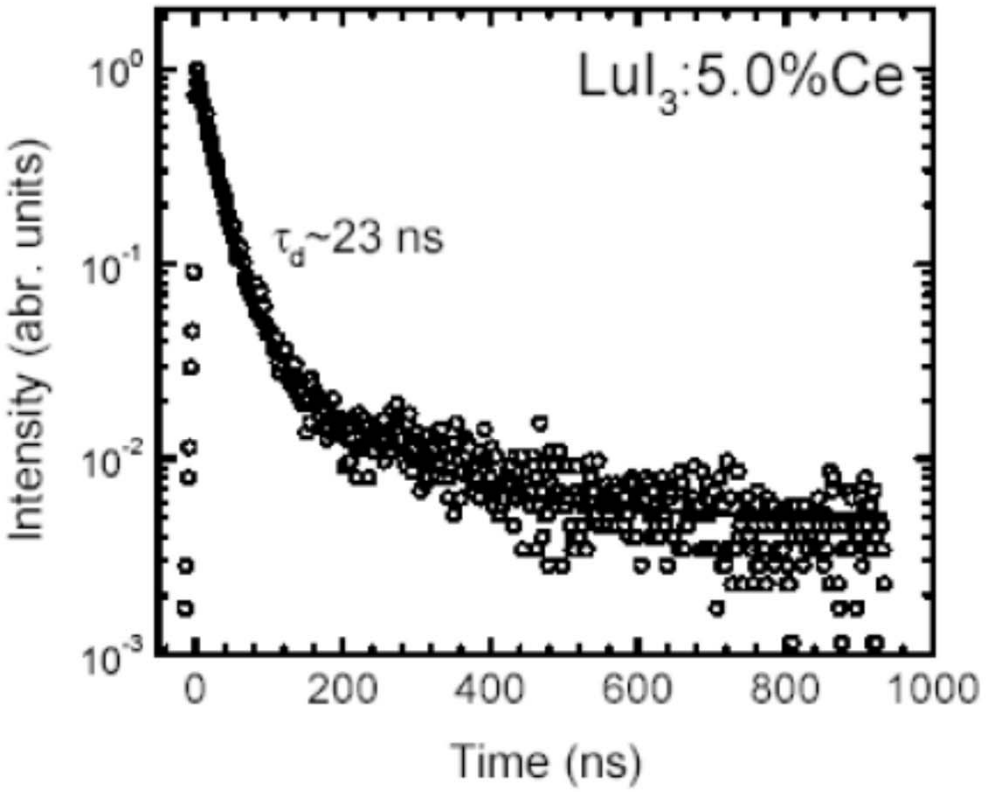

- ρ = 5.6 g/cm^3
- τ = 23-34 ns
- Y = 33-55 10^3 ph/MeV
- R_{662} = not yet optimized

LY of 76 000 phot/MeV (shaping time 10 us) measured in *Birowosuto et al, IEEE TNS 52, 1114 (2005)*

Slow us components

From presentation of P. Dorenbos, KEK, Japan, Nov 11, 2003

Eu-doped binary halides

New security measures: need for mid density, ultrahigh LY and excellent energy resolution scintillators, to distinquish radioactive isotopes $\Rightarrow$ **SrI_2:Eu** re-invented (**Hofstadter, U.S. Pat. 3,373,279 2 (1968)**

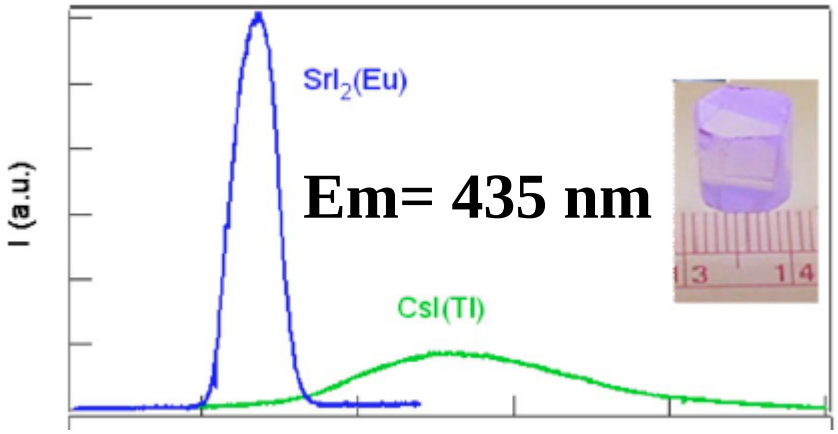

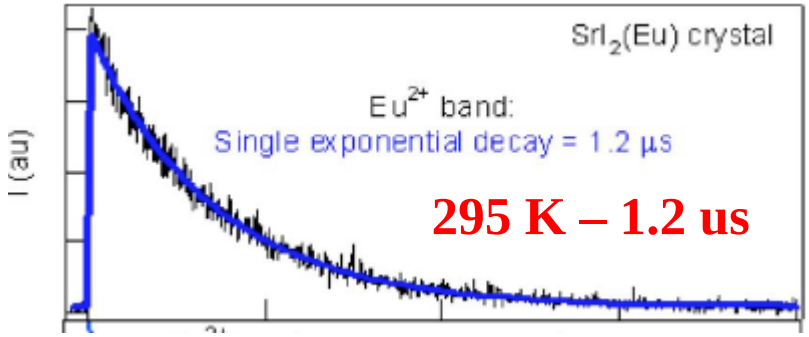

Cherepy et al, APL 92, 083508 (2008)
Yang et al, J.Lumin. 132,1824 (2012)

LY>80 000 phot/MeV, en.resolution 3.7%@667keV, however, hygroscopic, small Stokes shift results in reabsorption, DT size dep.

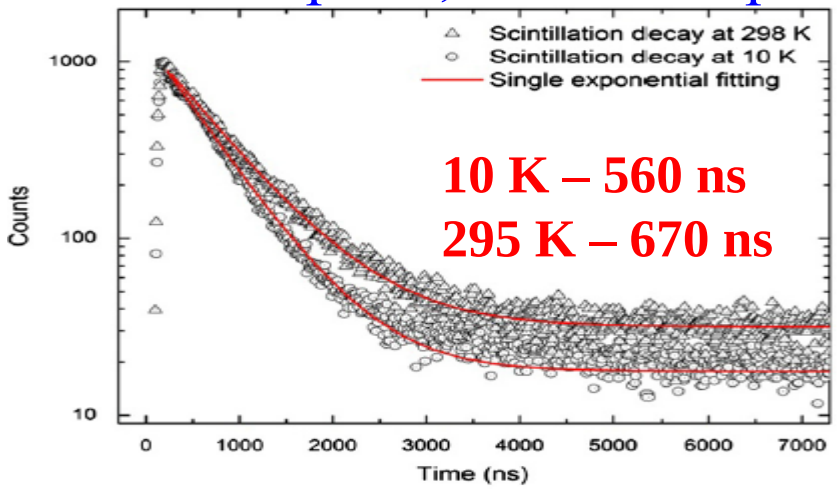

Eu-doped ternary halides/solid solutions

(Sr,Me)I_2:Eu: Me=Ba,Ca,Mg, Neal et al, NIM A 643, 75 (2011)
Cs(Sr,Ba)I_3:Eu: Wei et al, J.Cryst. Growth 384, 27 (2013)

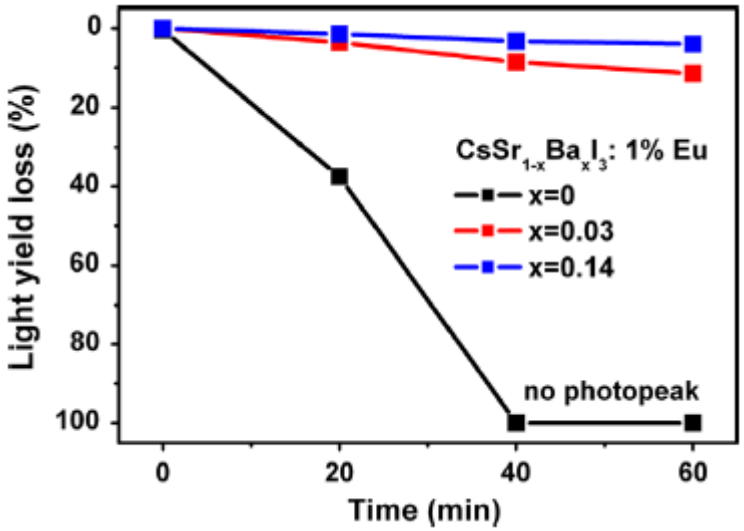

Substantial reduction of hygroscopicity after Ba admixture into CsSrI3:Eu
Moderate LY 26-28 000 phot/MeV, if Ba content is below 10at%.

Eu^{2+} is paramagnetic, a chance to use EPR for detailed study of its lattice site and perturbations around !

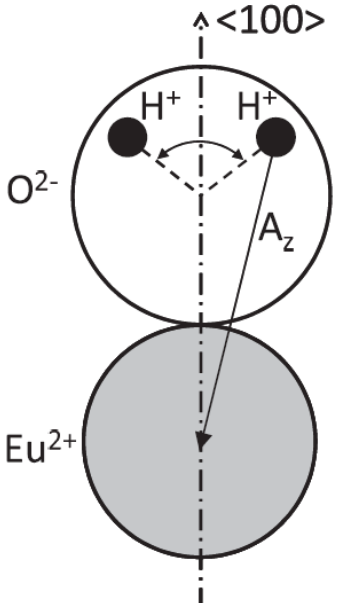

Eu^{2+} in CsBr is associated with H-containing impurity

Vrielinck et al, PRB 83, 054102 (2011)

SCINT2015: thermal neutrons for security applications

O4-1 Tl2LiYCl6 (Ce3+): New Tl-Based Elpasolite Scintillation Material
H. Kim,
O8-1 Development of Large Cs2LiLa(Br,Cl)6 Crystals for Nuclear Security Applications
R. Hawrami
O4-2 Lithium Alkaline Halides- Next Generation of Dual Mode Scintillators
L. Soundara-Pandian
O8-2 6LiInSe2 Scintillators for Neutron Radiography
E. Lukosi
O8-4 Luminescence and Scintillation Properties of Li4SiO4 Single Crystals for Neutron Scintillators
J. Pejchal
M1B-10 Single Crystal Growth of Cerium and Praseodymium Doped YCa4O(BO3)3 Scintillator by mPD Method
K. Kamada
M2C-6 Optimized Scintillators for Neutron Detection and Neutron Imaging
M. Morgano

7Li and 10B are Best isotopes for thermal neutron capture with high energy deposit from nuclear reaction in the form of particles, i.e. with short attenuation length!

Other Li-based elpasolites for neutron detection

Optical Materials 38 (2014) 154–160

Contents lists available at ScienceDirect

Optical Materials

journal homepage: www.elsevier.com/locate/optmat

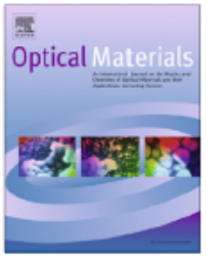

Two new cerium-doped mixed-anion elpasolite scintillators: $Cs_2NaYBr_3I_3$ and $Cs_2NaLaBr_3I_3$

Hua Wei [a,b,*], Luis Stand [a,b], Mariya Zhuravleva [a,b], Fang Meng [a,b], Victoria Martin [a,c], Charles L. Melcher [a,b]

[a] Scintillation Materials Research Center, University of Tennessee, Knoxville, United States
[b] Department of Materials Science and Engineering, University of Tennessee, Knoxville, United States
[c] Department of Nuclear Engineering, The University of Tennessee, Knoxville, United States

- LY of 58000 phot/MeV (Cs2NaLaBr3I3)
- Energy resolution 2.9%@662 keV
- Band gap 4.3-4.4 eV

Scintillation decay components and their ratios of $Cs_2NaLaBr_3I_3$: Ce and $Cs_2NaYBr_3I_3$.

	0.5% Ce	2% Ce	5% Ce	10% Ce	15% Ce
$Cs_2NaLaB_3I_3$					
Fast		83 (27%)	78 (25%)	57 (29%)	53 (33%)
Intermediate		322 (41%)	294 (40%)	247 (33%)	248 (39%)
Slow		1256 (32%)	1338 (34%)	1371 (38%)	1414 (28%)
$Cs_2NaYB_3I_3$					
Fast	64 (32%)	56 (47%)	48 (49%)	46 (46%)	
Intermediate	304 (38%)	284 (25%)	283 (18%)	287 (17%)	
Slow	1350 (30%)	2060 (28%)	2155 (33%)	2062 (37%)	

Cs_2HfCl_6 new halide scintillator

A. Burger et al. App. Phys. Let. 107 (2015) 143505

K. Saeki et al. App. Phys. Exp. 9 (2016) 042602

	Cs_2HfCl_6	Tl:NaI	Tl:CsI	Eu:SrI_2	Ce:$LaBr_3$
Density [g/cm^3]	3.8	3.4	4.5	4.6	5.3
m.p. [°C]	826	661	621	538	783
Zeff	58	50	51	49	47
Emission max. [nm]	400	410	540	430	360
Decay time [ns]	4,4 (95%); 300 (5%)	230	1100	600-2400	35
Light yield [ph/MeV]	54,000	38,000	66,000	80,000-120,000	61,000
Resolution [%] @662 eV	3-4	7	6	3-4	3
Hygroscopicity	low	yes	yes	yes	yes

Cs_2HfCl_6 crystal growth

Vertical Bridgman method

- Resistive furnace (2 segments)
- Container = **quartz ampoule**
- No seed
- pulling rate **0,2 - 1,0 mm/h**
- Temperature gradient **30 - 40 K/cr**
- Cooling rate **12 K/h**
- **10 days (heating, growth, cooling**

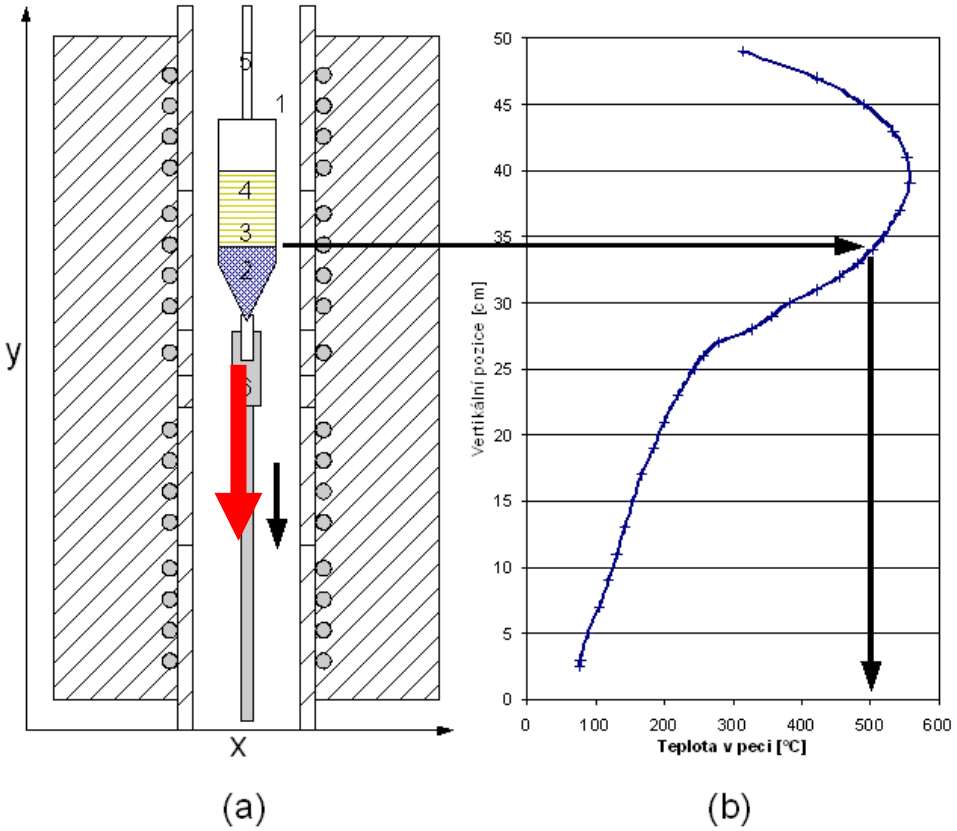

(a) (b)

Cs_2HfCl_6 – single crystal

Grown in Prague!

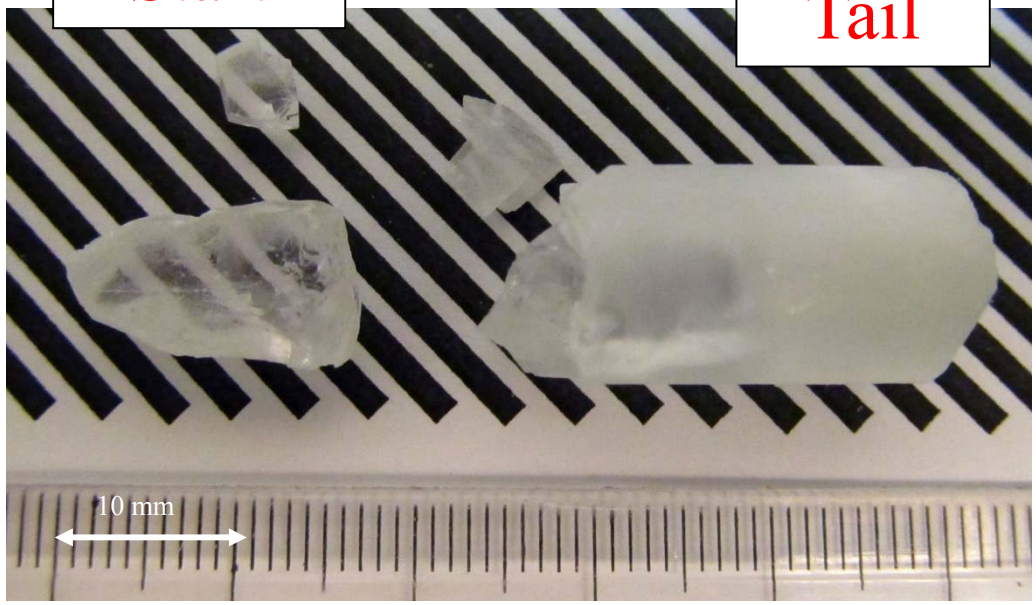

- 12 x 40 mm (D x L), colorless
- polycrystalline, homogeneous grains
- tip and bulk – transparent
- end – nontransparent

Radioluminescence spectra (X-ray)

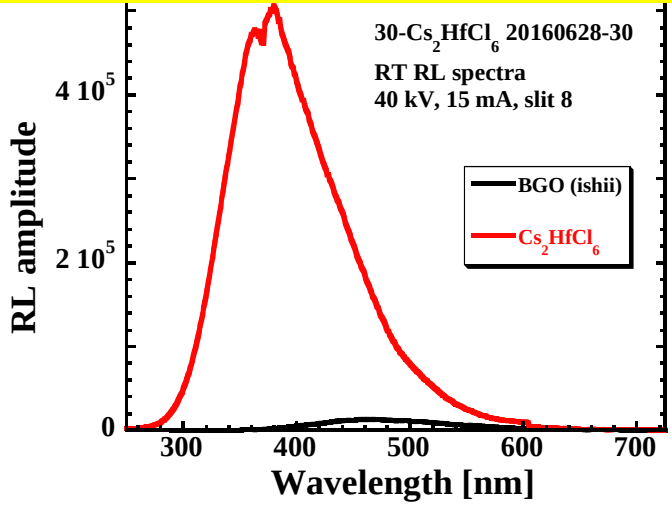

Crystal in quartz ampoule

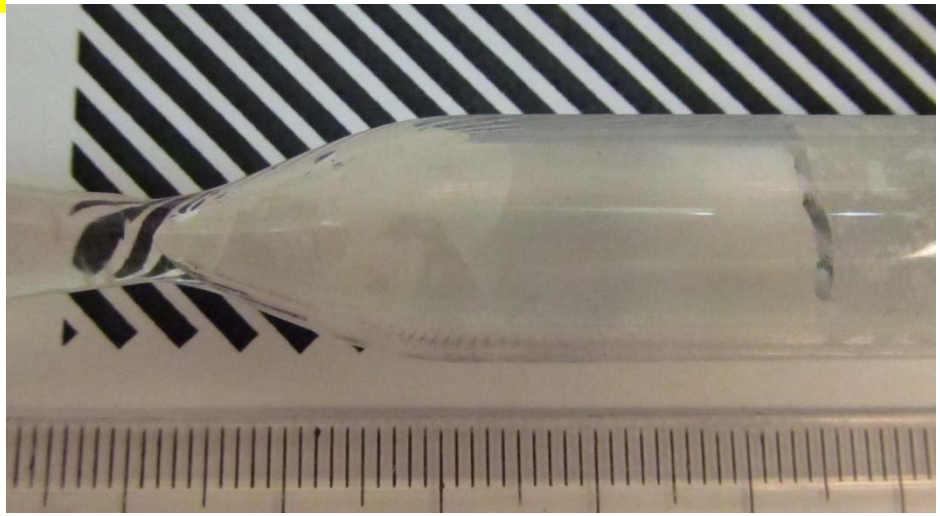

Cs_2HfCl_6 Photoluminescence characteristics

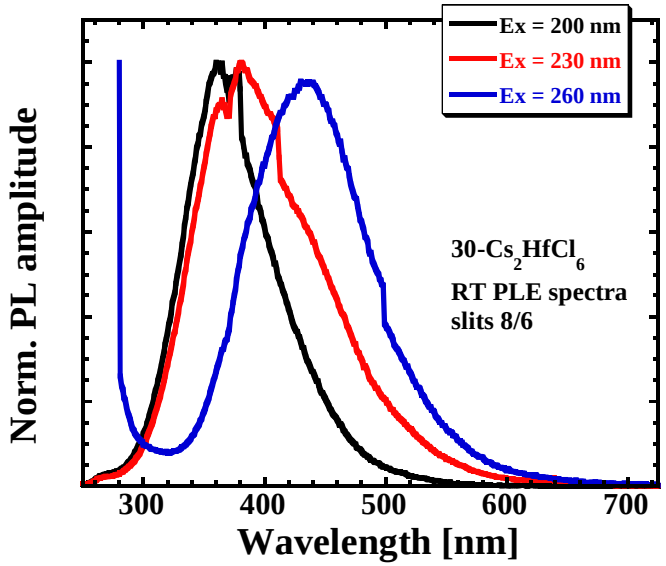

Intrinsic 360 nm and defect-related 440 nm bands
Microsecond decay times, still OK for homeland security applications

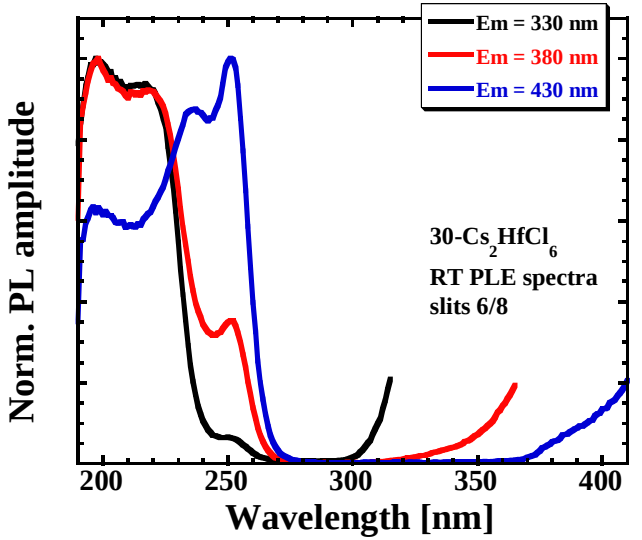

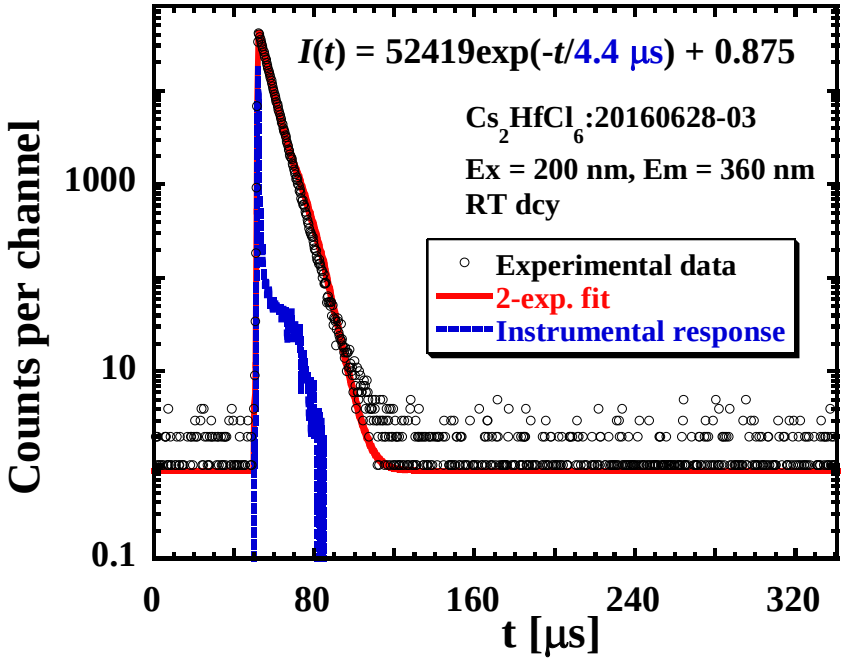

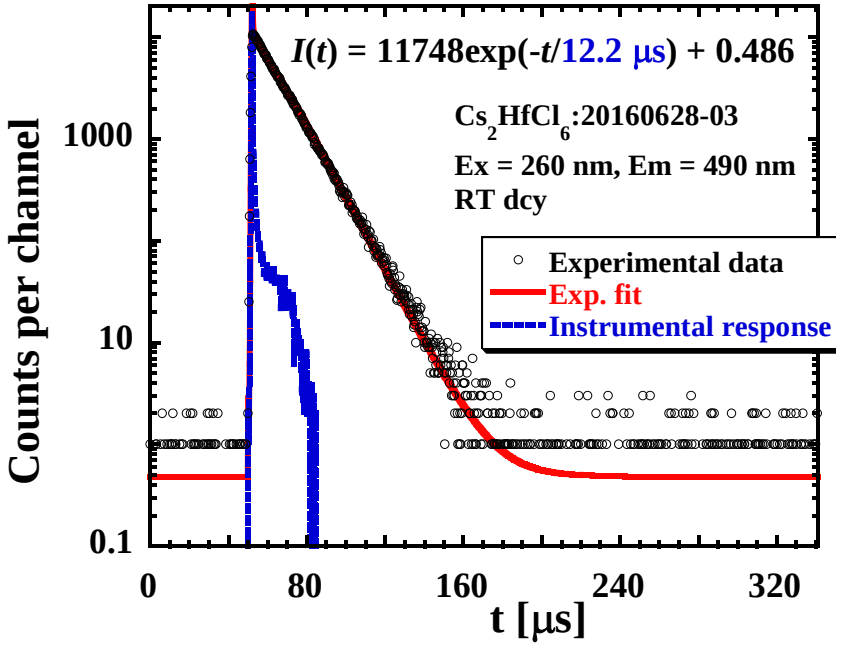

Energetic resolution and nonproportionality in scintillators – pulse height spectroscopy

- Light flash from scintillator due to HE photon absorption is converted into current pulse in PMT output which is integrated in a time window = collected charge. Its amount is equivalent to a number of photoelectrons generated at PMT photocathode
- Given the signal amplitude, +1 is added to an appropriate channel of multichannel analyser and measurement cycle is repeated
- Measuurement of
  - Photoelectron yield (Nphels)
  - Light yield
  - FWHM (=energy resolution)
  - Nonproportionality (Nphels(Ein))

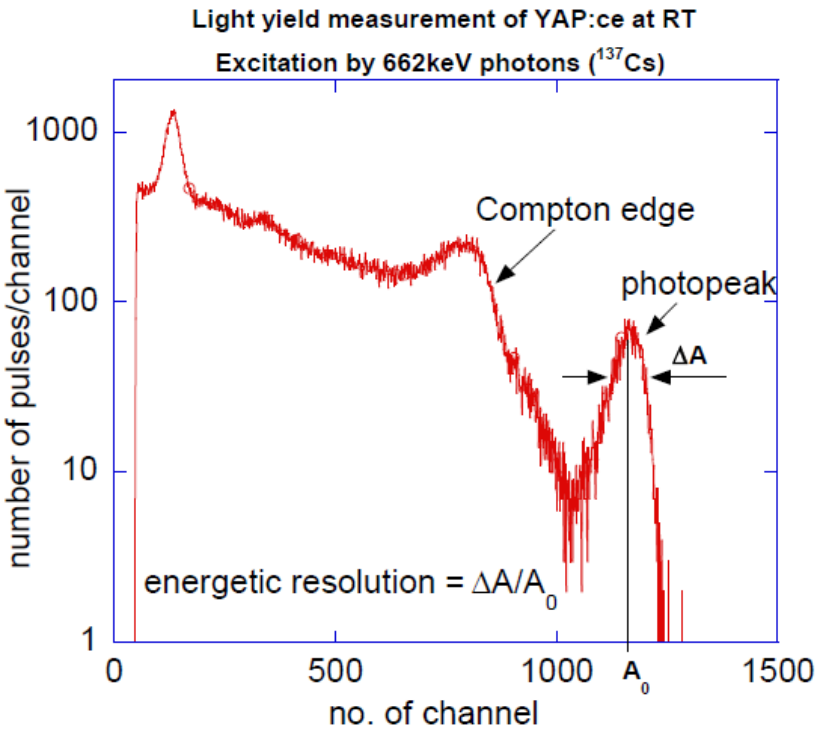

Components of energy resolution

The energy resolution (ΔE/E) of a full energy peak measured with a scintillator coupled to a photomultiplier (PMT) can be written as

$$(\Delta E/E)^2 = (\delta_{sc})^2 + (\delta_p)^2 + (\delta_{st})^2$$

where **δsc** is the intrinsic resolution of the crystal, **δp** is the transfer resolution and **δst** is the statistical contribution of PMT to the resolution.

$$\delta st = (2.355/N^{1/2}) \times (1 + \varepsilon)^{1/2}$$

where **N is the number of the photoelectrons** and ε is the variance of the PMT gain

*Sreebunpeng et al, Nucl. Instr. Meth. Phys. Res. B **286**, 85 (2012)*

Examples of BGO versus LSO:Ce

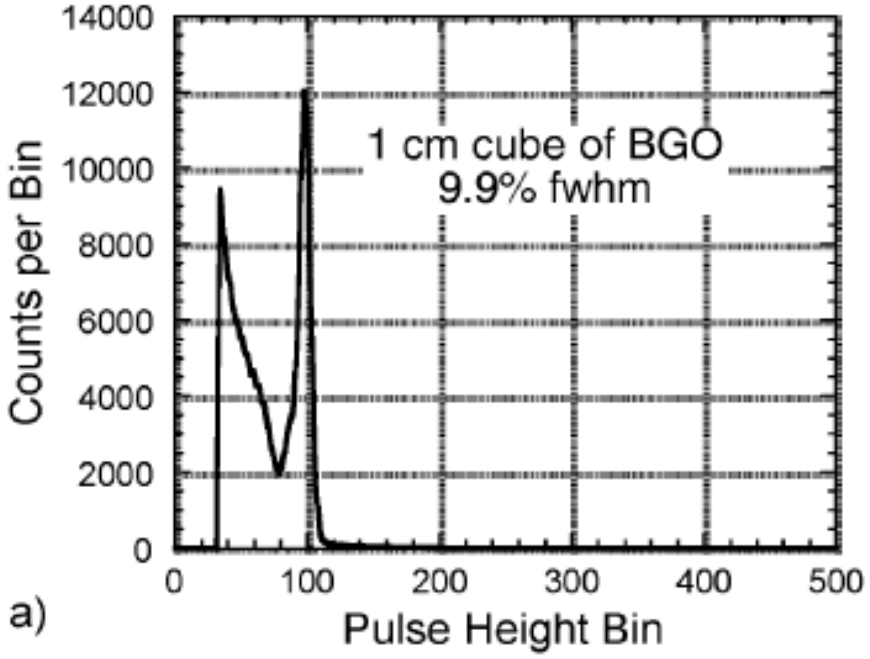

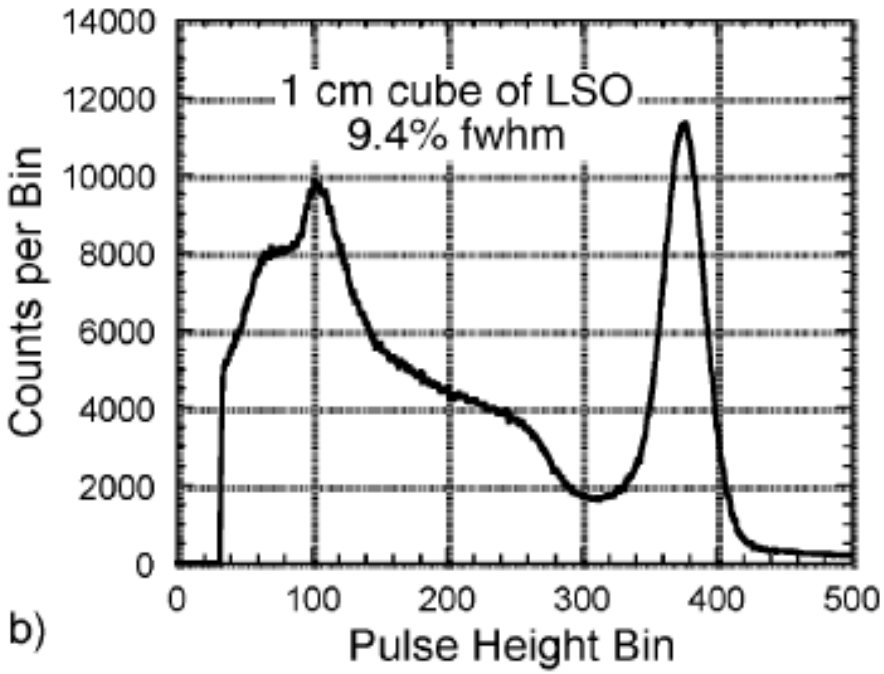

LY of BGO approx. 8000 phot/MeV

LY of LSO:Ce approx. 30 000 phot/MeV

δst is approx. 2x smaller in case of LSO:Ce, but energy resolution is comparable ⇒ δsc must be comparatively bigger in LSO:Ce!

The reason is nonproportionality (and eventually material inhomogeneity and defects/traps as well)

Rooney, Valentine, IEEE Trans. Nucl. Sci., 43, 1271 (1996)

Nonproportionality = energy dependence of LY

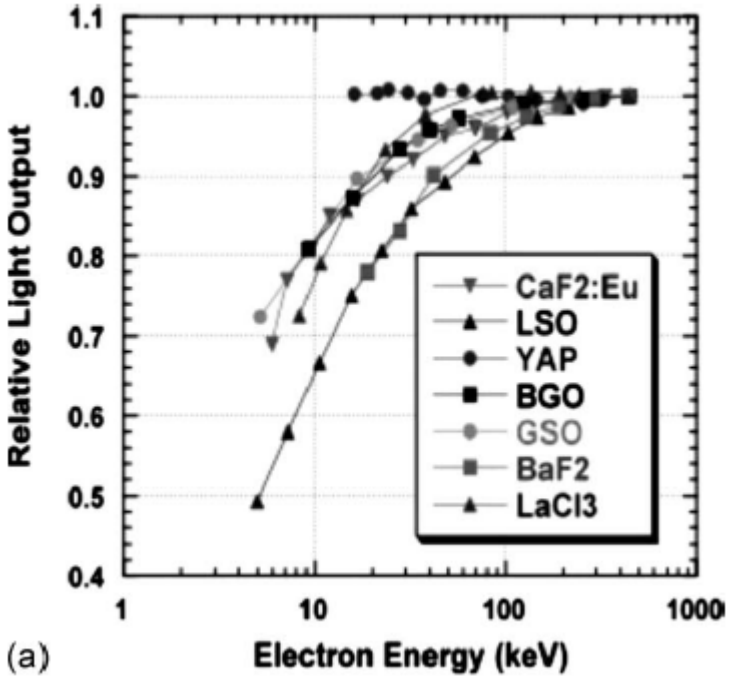

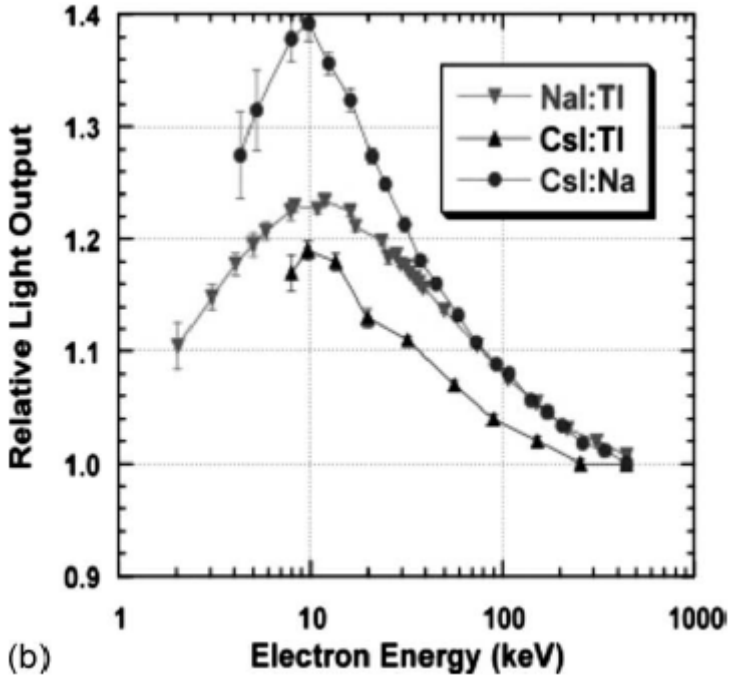

Towards lowest energies LY value is always decreasing – why?

Moses, IEEE TNS 55,1049 (2008) – history and problem survey

Deposited energy in a unit volume versus LY

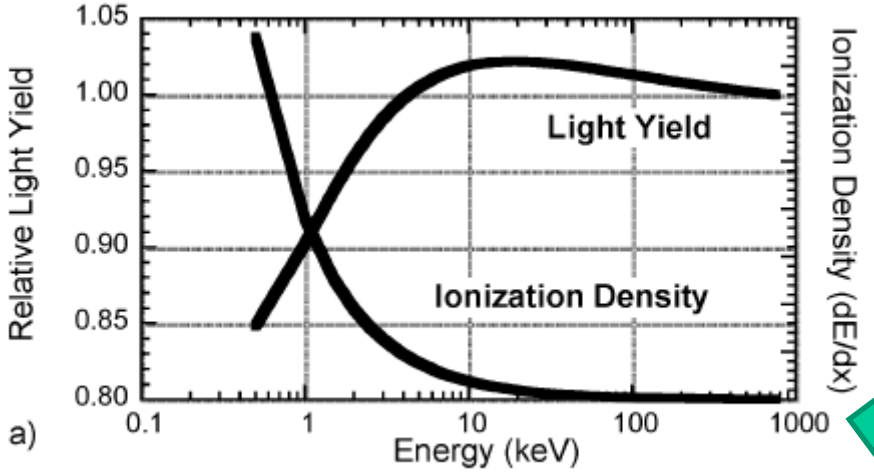

Closely spaced elementary excitations in the latice ANNIHILATE Without producing photons!

e.g. two excitons nearby will interact and as a result only one (or none) exciton state will remain, the rest of energy will be converted to phonons

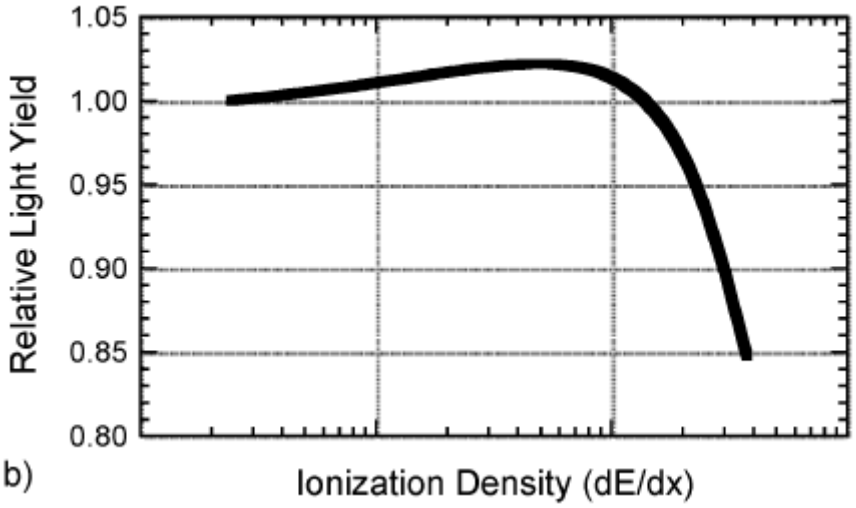

Moses et al, IEEE TNS 55, 1049 (2008)

An analytical model of nonproportional scintillator light yield in terms of recombination rates

$$-\frac{dn_{ex}(x)}{dt} = (R_{1x}+K_{1x})n_{ex}(x) + (R_{2x}+K_{2x})n_{ex}^2(x) - \gamma_{ex}n_{eh}(x) + \gamma_{xe}n_{ex}(x) + K_{3x}n_{ex}(x)^3 - f_x n(x)\delta(t),$$

$$-\frac{dn_{eh}(x)}{dt} = (R_{1eh}+K_{1eh})n_{eh}(x) + (R_{2eh}+K_{2eh})n_{eh}^2(x) - \gamma_{xe}n_{ex}(x) + \gamma_{ex}n_{eh}(x) + K_{3eh}n_{eh}^3(x) - (1-f_x)n(x)\delta(t),$$

Densities n of excitons (ex) or electron-holes (eh) along the track (one dimensional case), R and K are rate constants of radiative and nonradiative(quenching) recombinations.

Total density of excitation is then $n(x)=n_{ex}(x)+n_{eh}(x)$,

Accordingly, $n(x) = (-\delta E/\delta x)/(\pi r^2 E_{eh})$

where E is the total initial energy incident at any point x, $r2$ is the average area of cross section of the track, and Eeh is the average energy required to create an excitation in a scintillator,

Bizarri et al, J. Appl. Physics 105, 044507 (2009)

Local (relative) LY

$$Y_L = \frac{R_{1x}\langle n_{ex}(x)\rangle + R_{2x}\langle n_{ex}^2(x)\rangle + R_{1eh}\langle n_{eh}(x)\rangle + R_{2eh}\langle n_{eh}^2(x)\rangle}{n(x)},$$

$$Y_L = \frac{a_1 + a_2 n(x)}{1 + a_3 n(x) + a_4 n(x)^2},$$

Because of $n(x)^2$ in denominator, starting from some critical density $n_c(x)$, the value of light yield Y_L will start to monotonically decrease!

Energy dependence of energy deposit in a unit volume

Stopping power given by the modified (nonrelativistic) Bethe equation[18] is

$$-\frac{dE}{dx}=\frac{2\pi e^4\kappa^2\rho_e}{E}\ln\left\{\left(\frac{2.71}{2}\right)^{1/2}[(E+0.81I)/I]\right\}, \qquad (12)$$

where $\kappa=(4\pi\varepsilon_0)^{-1}=8.9877\times10^9$, E is the total initial incident energy of gamma rays at any point x along its track, I is the average ionization energy, and ρ_e is the electron density

With decreasing incident energy E the energy deposit in unit volume is increasing!

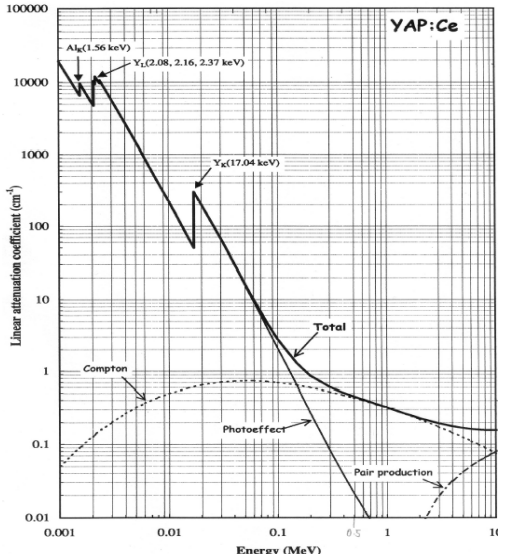

Model of LY energy dependence

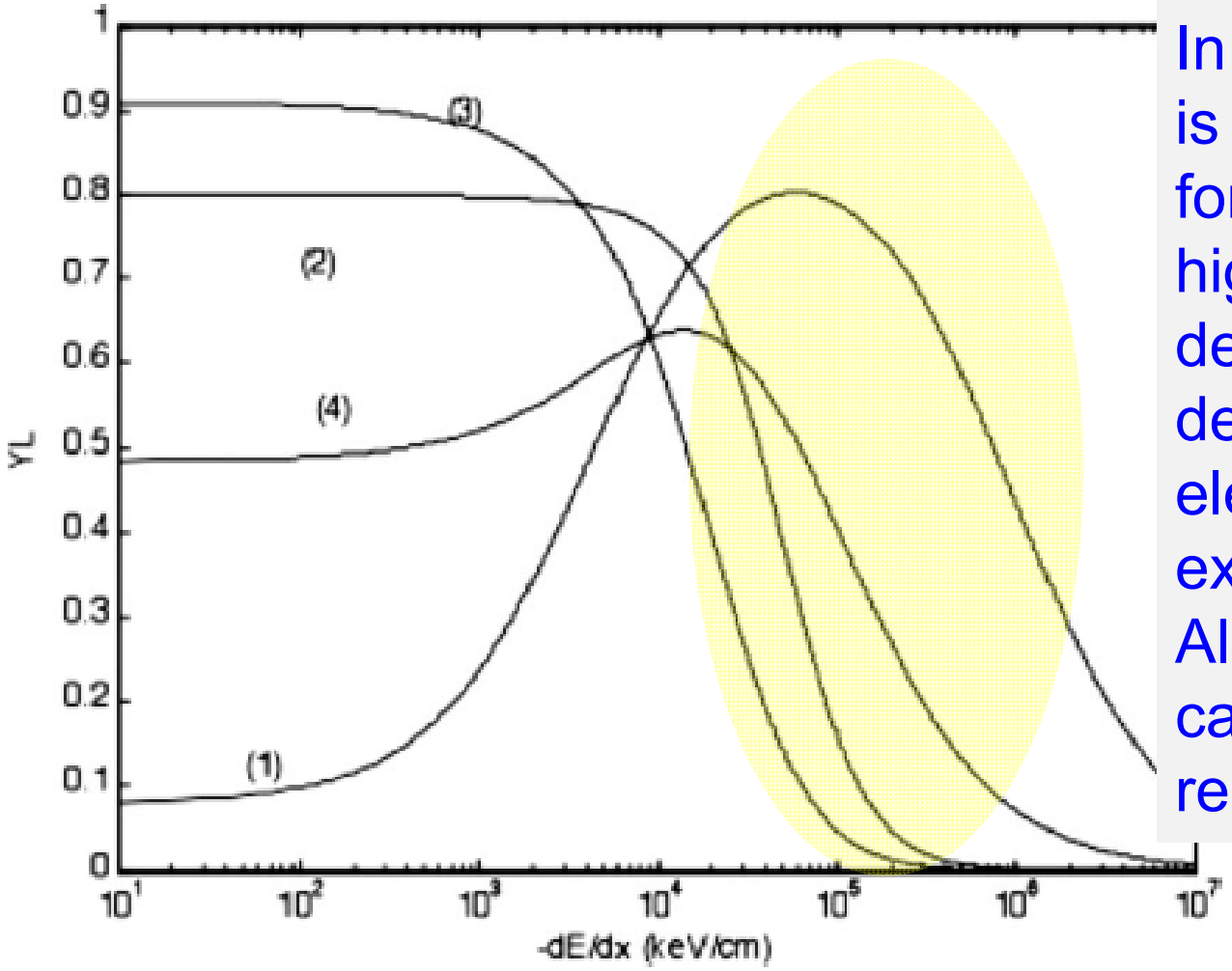

In all cases YL is decreasing for sufficiently high energy deposit, i.e. density of elementary excitations
Also the hump can be reproduced.

FIG. 2. (a) The local light yield (Y_L) plotted as a function of ($-dE/dx$) (keV/cm) from Eq. (8) for NaI:Tl (1), BaF_2:Ce (2), GSO:Ce (3), and $LaCl_3$:Ce (4). Rates used for different materials are given in Table I.

The roles of thermalized and hot carrier diffusion in determining light yield and proportionality of scintillators

Numerical modeling and comparison to experiment in the materials for which suitable parameters have been measured confirm that three of the most important material parameters for predicting proportionality and the related host-dependent light yield (LY) of scintillators are (i) the carrier diffusion coefficients (including hole self-trapping if present, and hot-electron diffusion if unthermalized), (ii) the kinetic order and

Competition of 2nd order quenching and diffusion

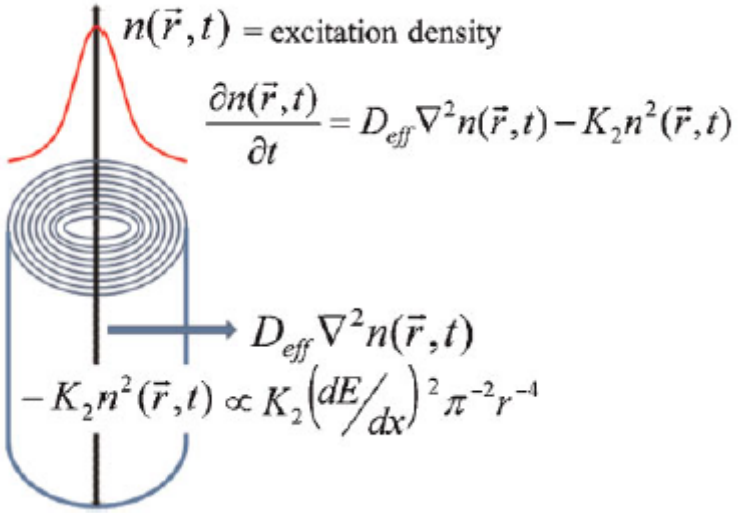

associated rate constant of nonlinear quenching, and (iii) deep-trapping probability. Thermalized carrier diffusion appears sufficient to describe the main trends in oxides and semi-conductors. For heavier halide hosts, it appears necessary to take account of hot-electron diffusion to explain several important host-dependent trends.

Role of carrier diffusion

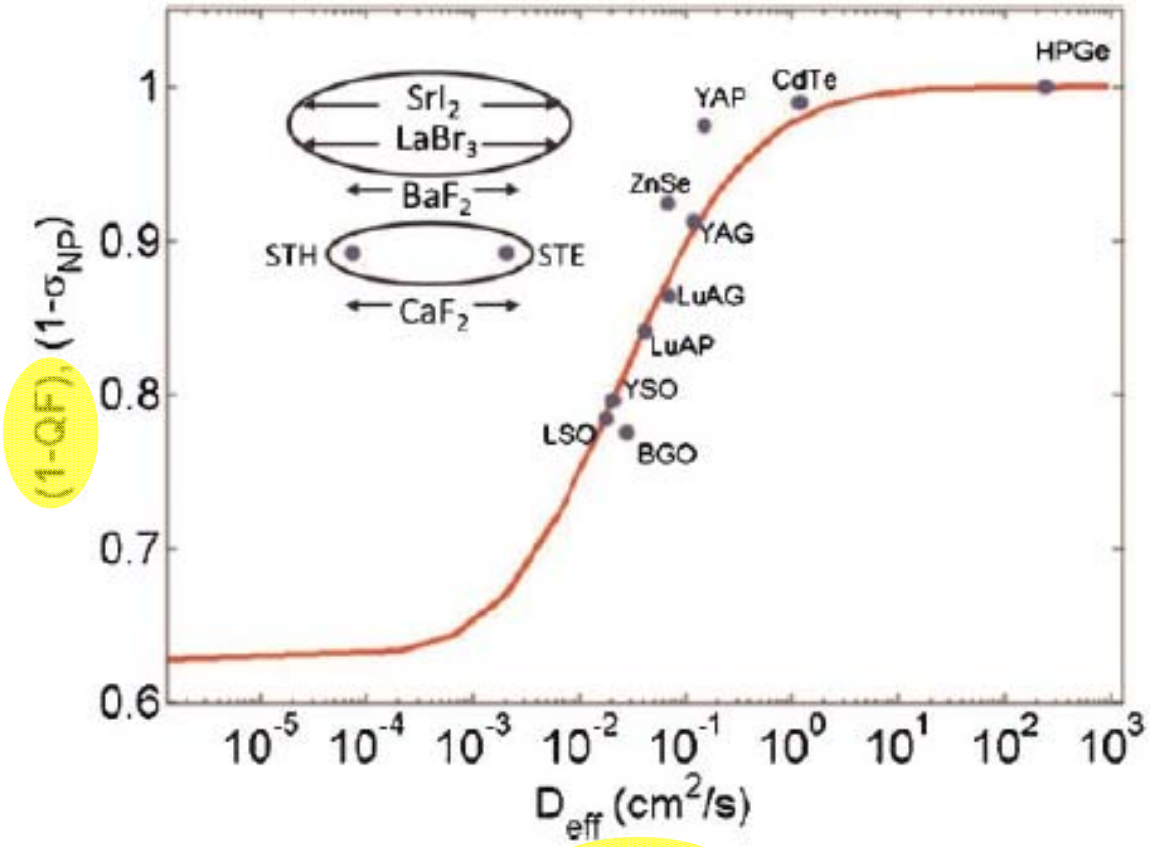

The solid red curve plots results of survival against the model of nonlinear quenching in Fig. 1 evaluated for r0=3 nm, t_{NLQ}=10 ps, $n0_{excited}$=10^{20} e-h cm^3 as a function of ambipolar diffusion coefficient Deff. [2].
The points plot empirical $1-\sigma_{NP}$ measures of energy dependent LY (or collected charge in CdTe and Ge) versus D_{eff} computed for each material from band effective mass.

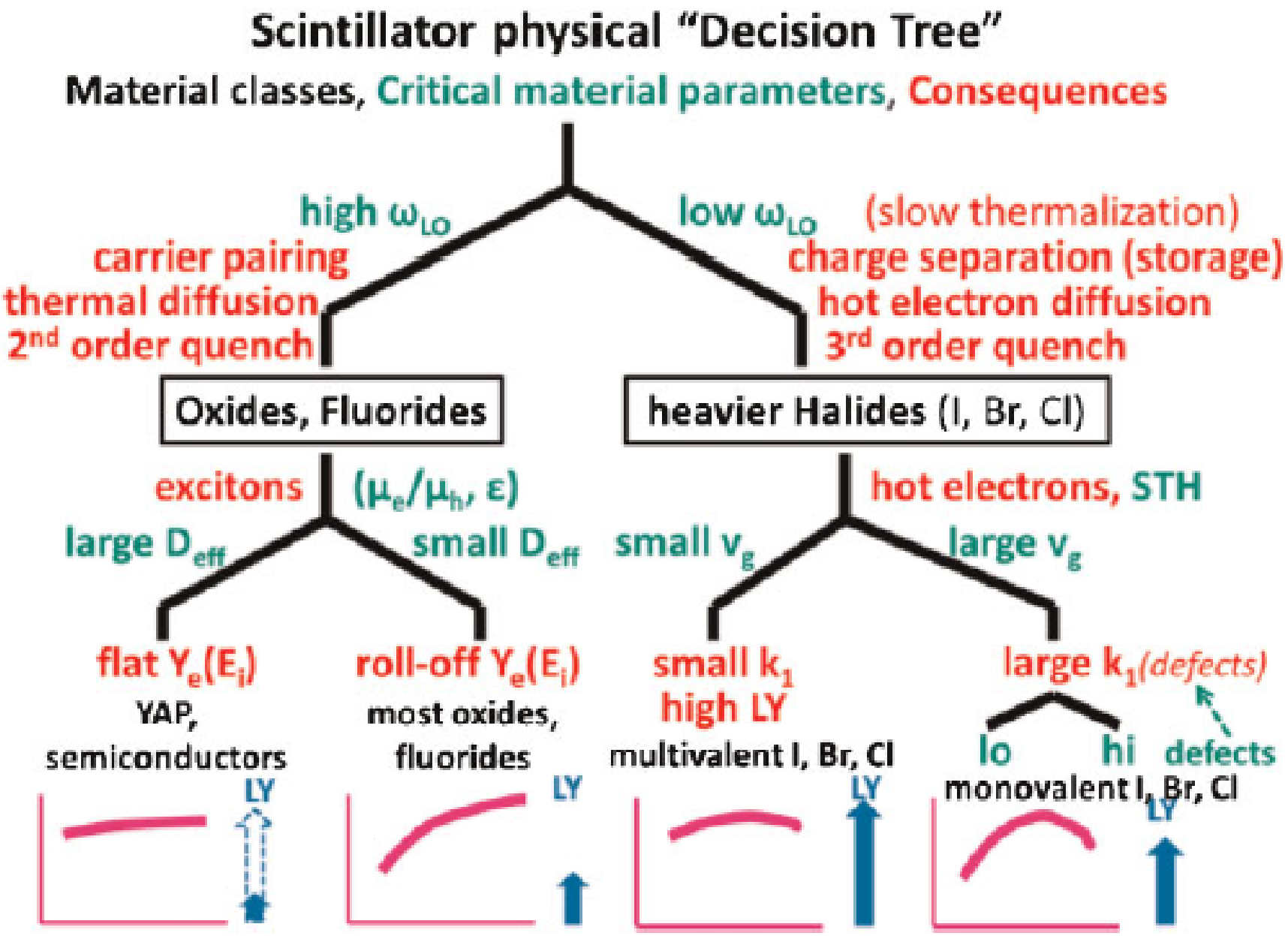

Grim et al, Phys. Stat. Sol. A ***209****, 2421 (2012)*

Conclusions

- Halides are often hygroscopic, less mechanically robust, with much lower melting temperature compared to oxides
- Preparation technology requires to avoid the contact with air and humidity
- Smaller band gap (bromides, iodides) compared to oxides makes them interesting from the efficiency point of view
- Energy transfer towards emission centers is often different, host excitonic states might be more important
- Modern halide scintillators are superior especially in terms of energy resolution so that the detailed understanding of its bottlenecks and optimization recipes are of high interest
- Driving forces for both oxide&halide scintillator development will come from medical, HEP, and high-tech industrial applications, security measures, space technology

Financial&networking support acknowledged from:

ASCIMAT

Czech science foundation no. P202/12/0805, 15-18300Y and 16-15569S. MEYS LH14266 and SAFMAT LM2015088 and LO1409. EC H2020 no. 644260 (Intelum) and no. 690599 (Ascimat). Crystal Clear Collaboration, COST FAST TD1401.

Materials Views
www.MaterialsViews.com

ADVANCED OPTICAL MATERIALS
www.advopticalmat.de

Recent R&D Trends in Inorganic Single-Crystal Scintillator Materials for Radiation Detection

Martin Nikl and Akira Yoshikawa*

Adv. Opt. Mater. **3**, 463–481 (2015).